The Analysis of Seasonally Varying Flow in a Crystalline Rock Watershed Using an Integrated Surface Water and Groundwater Model

by

Jefferey Ernest Randall

A thesis
presented to the University of Waterloo
in fulfillment of the
thesis requirement for the degree of

Master of Applied Science
in
Civil Engineering

Waterloo, Ontario, Canada, 2005

I hereby declare that I am the sole author of this thesis.

This is a true copy of the thesis, including any required final revisions, as accepted by my examiners. I understand that my thesis may be made electronically available to the public.

ABSTRACT

Researchers, explorers, and philosophers have dedicated many lifetimes attempting to discover, document, and quantify the vast physical processes and interactions occurring in nature. Our understanding of physical processes has often been reflected in the form of numerical models that assist academics in unraveling the many complexities that exist in our physical environment. To that end, integrated surface water-groundwater models attempt to simulate the complex processes and relationships occurring throughout the hydrologic cycle, accounting for evapotranspiration and surface water, variably saturated groundwater, and channel flows.

The Bass Lake watershed is located in the Muskoka district of Ontario, within a crystalline rock environment consistent with typical Canadian Shield settings. Numerous data collection programs and methods were used to compile environmental and field-scale datasets. The integrated surface water-groundwater model, HydroGeoSphere (Therrien et al., 2005), was used for all Bass Lake watershed simulation models.

Simulation results were compared to expected trends and observed field data. The groundwater heads and flow vector fields show groundwater movement in expected directions with reasonable flow velocities. The subsurface saturation levels behave as expected, confirming the evapotranspiration component is withdrawing groundwater during plant transpiration. The surface water depths and locations of water accumulation are consistent with known and collected field data. The surface waters flow in expected directions at reasonable flow speeds. Simulated Bass Lake surface elevations were compared to observed surface water elevations. Low overland friction values produced the most accurate Bass Lake elevations, with high overland friction values slightly overestimating the Bass Lake water level throughout the simulation period. Fluid exchange between surface water and groundwater domains was consistent with expected flux rates. The integrated surface water-groundwater model HydroGeoSphere ultimately produced acceptable simulations of the Bass Lake model domain.

ACKNOWLEDGEMENTS

I would like to extend special thanks to the following people:

- to Dr. Jon F. Sykes, who gave me the opportunity to work on this project, who funded me, and who guided me throughout its completion

- to Stefano Normani, for his wealth of knowledge, his computer skills, and for dealing with a multitude of questions, comments, and concerns

- to Rob McLaren, for solving many of my HydroGeoSphere source code issues and without whom, my models would never have completed

I would like to extend additional thanks to the following people:

- to Terry Ridgway, for his field work experience and willingness to offer help whenever it was needed

- to Young-Jin Park, for solving the ET source code issue, allowing the completion of this thesis

- to Margo, Moggs, Scooter, and Mareky, who were always up for a break, some food, a coffee, or just some laughs

- to the numerous "Bass Lake Taxi" drivers without whom the field sampling program would not have been possible

I would also like to thank those who were there throughout the project:

- to Meghan, for supporting me, for listening to me, and most importantly, for making me laugh and smile

- to Mum, Dad, and Brad, for offering support, consolation, and for simply always being there for me

TABLE OF CONTENTS

LIST OF TABLES

LIST OF FIGURES

Chapter 1

Introduction

The natural environment, with its complex inner workings, behaves in a seemingly effortless fashion. Researchers have dedicated many lifetimes trying to discover, document, and quantify the vast physical processes and interactions occurring in nature. However, regardless of how well these physical relationships are understood, the complex interactions taking place throughout nature are difficult to simulate and even more difficult to predict.

Lakes, ponds, rivers, and streams are visible expressions of overland flow. Maintenance of their quality and quantity has become a major concern throughout the past few decades, with many of the external environmental stresses placed on surface waters related to human activities. Despite limited visibility of groundwater resources, their quality and quantity have also been under increasing human stresses and have become a focus of many governing bodies around the world. Understanding the complexity of the surface and subsurface flow processes, evapotranspiration, and the interactions between

them, more commonly referred to simply as the hydrologic cycle, is a complicated challenge.

The Muskoka district of Ontario (Figure 1.0.1) is located on the Canadian Shield region and is characterized by vast forests, multiple lakes, and minimally impacted natural settings. Due to its status as a popular vacation destination, the quality and quantity of both surface water and groundwater in the Muskoka district are of major concern for area communities. The application of an integrated surface water-groundwater model to a crystalline rock environment (as is consistent with Canadian Shield settings) would offer insights and information that could help examine the existing water quality, water quantity, and provide interpretations of human impact.

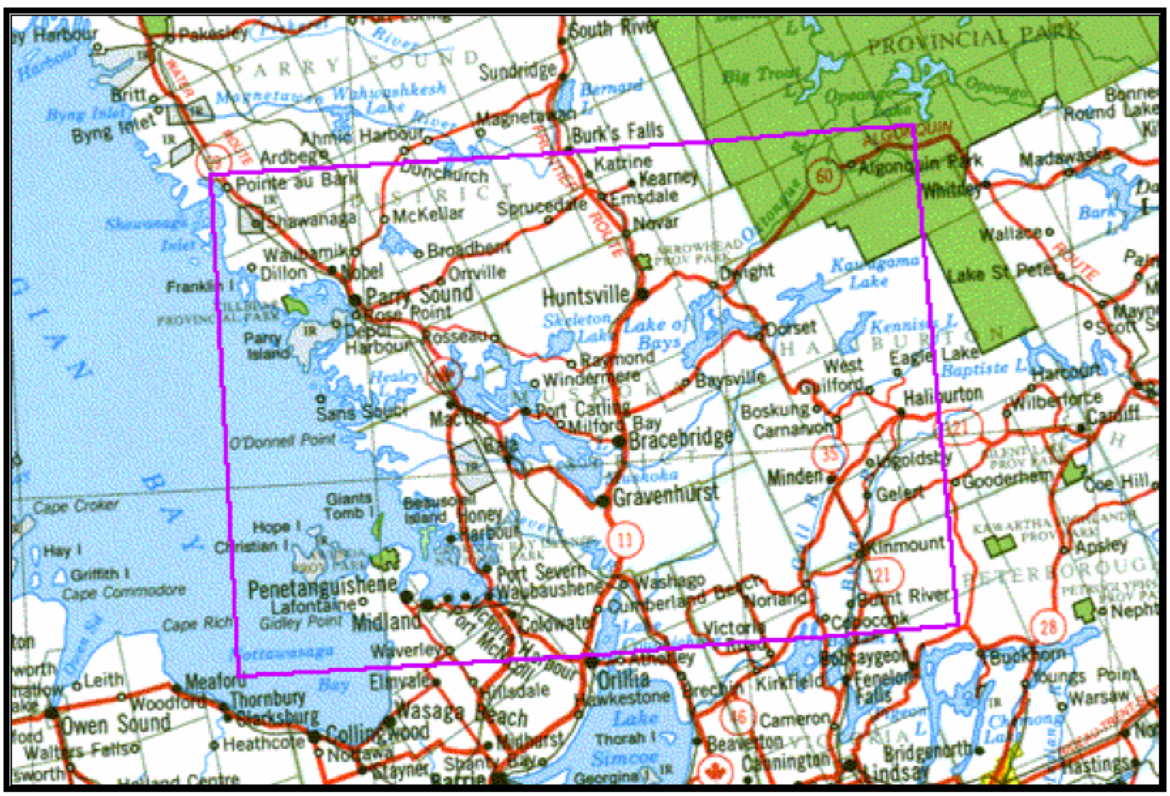

Figure 1.0.1 – Muskoka District Location (Randall et al., 2003)

1.1 PROJECT OBJECTIVE AND SCOPE

The objective of this thesis is to simulate and analyze seasonally varying groundwater and surface water flow within a crystalline rock environment. To accomplish this, a physically-based, integrated surface water-groundwater numerical model will be applied to the Bass Lake watershed, located within the Muskoka district. This model incorporates all components of the hydrologic cycle: surface water flow, saturated groundwater flow, unsaturated groundwater flow, and evapotranspiration.

Additionally, this analysis will test the applicability of an integrated surface water-groundwater model currently in development at the University of Waterloo. The Bass Lake watershed is the first large-scale model incorporating all hydrologic components to be simulated using the HydroGeoSphere model (Therrien et al., 2005). The construction and simulation of the Bass Lake watershed model will provide valuable feedback to the model development team throughout the model application stage.

Finally, this thesis will compile a large climatological and physical property database for the Bass Lake watershed and surrounding model domain. This database will facilitate future studies of the watershed, including possible contaminant transport and dual continuum fractured-flow modelling.

Chapter 2

Integrated Surface Water – Groundwater Simulation Models

In nature, the hydrologic cycle is never-ending. Water evaporates from soil, rivers, lakes, and oceans, transpires from plants, and sublimates from snow and ice. The water vapour accumulates in the atmosphere and returns to the ground as rain, sleet, and snow. It then flows and accumulates as surface water or infiltrates the subsurface to become groundwater. This groundwater then returns to surface water through lake and river baseflow (Figure 2.0.1).

Numerical simulation of the hydrologic cycle (Figure 2.0.1) must account for all known dominant physical processes occurring within nature. A conceptual model of the physical processes, known integrated model limitations, and existing simulation models will be discussed in this Chapter.

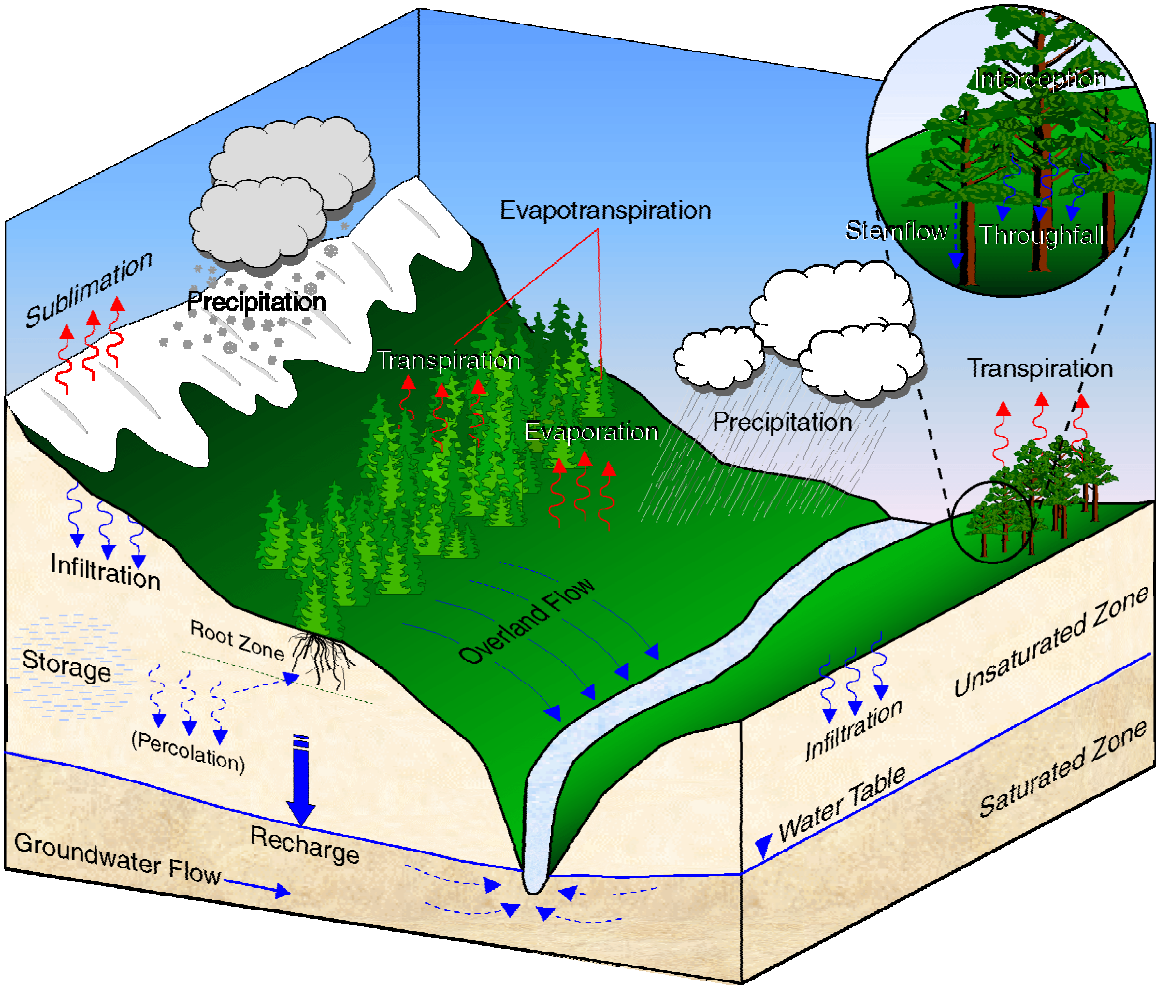

Figure 2.0.1 – Hydrologic Cycle (with permission from Jyrkama, 2003)

2.1 Integrated Model Conceptualization and Limitations

Freeze and Harlan (1969) proposed a blueprint (FH69) for integrated surface water-groundwater models, detailing the physical processes and the governing partial differential equations occurring therein. A conceptual flow chart of the relationships between the physical processes is presented in Figure 2.1.1.

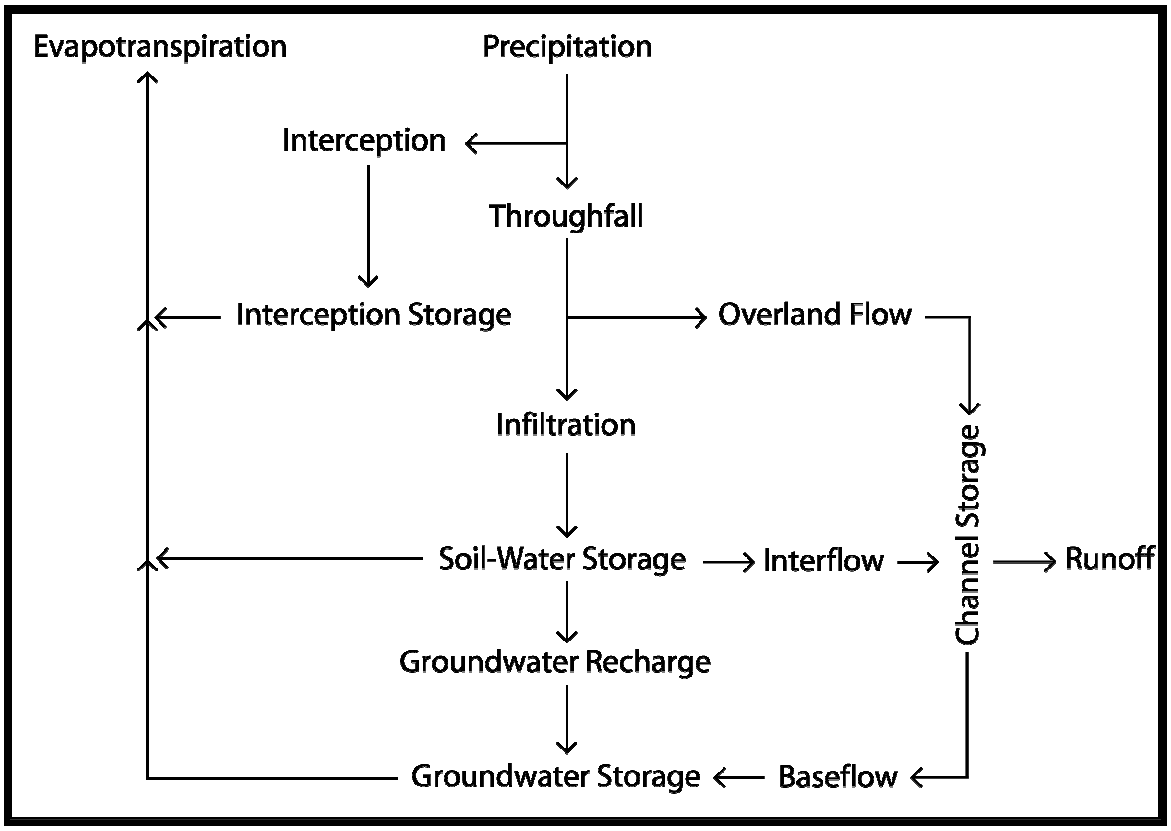

Figure 2.1.1 – Conceptual Integrated Surface Water-Groundwater Model (Freeze & Harlan, 1969)

Since the development of the FH69 blueprint, various concerns related to integrated surface water-groundwater modelling have been presented by the scientific community. Keith Beven (1996a) acknowledges the practical applicability of integrated models in predicting surface water and groundwater flow; however, he is concerned with the formulations of distributed models and their ability to realistically describe the hydrologic processes.

Beven's concerns are largely related to the validity of the flow equations used in distributed models. These concerns include the simplifying assumptions required for flow solution development, the availability of field-scale parameter estimates, and model non-uniqueness resulting from numerous required input parameters. He believes these concerns should be addressed to increase the validity of the FH69 blueprint.

These limitations have been addressed and further discussed by Refsgaard et al. (1996) and by Beven (1996b). Graham and Butt (2005) argue that the major limitations of integrated simulations are similar to those expressed by Beven (1996a):

- High data acquisition costs resulting from numerous required input parameters
- Increased model simulation times resulting from increased model complexity
- Model over-parameterization resulting from increased model input requirements
- Physics-based model representing field-scale parameters with mathematical descriptions valid only for laboratory-scale experimental conditions

A comprehensive understanding of integrated surface water-groundwater model limitations is required prior to model design and construction. Many of the concerns regarding integrated models are similar to those found in independent surface or groundwater models; it is therefore apparent that any simulation model will contain some degree of uncertainty. Additionally, advances in computer technology continue to decrease simulation times and improve integrated model efficiency and applicability.

2.2 EXISTING INTEGRATED GROUNDWATER – SURFACE WATER MODELS

At present, several mathematical models exist that are capable of simulating the integrated surface water-groundwater flow interactions of the complete hydrologic cycle. These models may take different approaches in solving the combined surface water and groundwater flows, but all offer significant contributions to the future of watershed management and protection. Four of the most prolific and contemporary models and their methodologies are discussed in sections 2.2.1 to 2.2.4.

2.2.1 MIKE SHE

The integrated simulation model MIKE SHE emerged from the development of two independent simulation models. The integrated model Système Hydrologique Européen (SHE) (Abbott et al., 1986) was coupled with the MIKE 11 channel flow model (Havnø

et at., 1995) by the Danish Hydrologic Institute (DHI) to create the MIKE SHE coupled surface water-groundwater model. The physically-based distributed numerical model uses a finite difference approach to simulate surface water flow, groundwater flow, and channel flow regimes. The 3-dimensional groundwater flow is calculated using the Darcy equation. The unsaturated groundwater flow can be calculated using the Richards equation or by using a simplified gravity flow approach (assumes 1-dimensional vertical flow, ignores capillarity). The overland flow is calculated using a diffusion wave equation while the exchange flux is determined using a head difference method (Graham & Butts, 2005). The channel flow can be calculated with several different methods, including a 6-point Abbott-Ionescu method (Havnø et. Al, 1995) or a quasi-steady state approximation method.

This coupled model is solved using an iterative implicit finite difference approach. This approach solves the surface water and groundwater components separately and uses the resulting head values to determine the exchange flux through the unsaturated zone. The model simulates the surface and groundwater flows separately, and is therefore cannot be considered fully coupled. The model is limited to surface grids with equal-area square elements in the x- and y- directions. (Havnø et al., 1995)

2.2.2 InHM

The Integrated Hydrologic Model (InHM) was developed by VanderKwaak (1999) at the University of Waterloo. InHM uses an integrated finite difference or an integrated finite element approach capable of simultaneously modelling the surface water and groundwater flow domains. InHM also offers the option of dual continua (fractured flow) groundwater flow simulation. The 3-dimensional variably saturated groundwater flow is calculated using the Richard's equation, while the overland flow is calculated using the diffusion wave and Manning's equations. The exchange flux between the surface water and groundwater flow domains is a function of the head difference between the two domains (VanderKwaak, 1999).

This fully-integrated model solves the overland, vadose zone, and groundwater flows simultaneously for each timestep but does not consider the evaporation or plant transpiration processes (VanderKwaak, 1999).

2.2.3 MODHMS

MODHMS is a MODFLOW (McDonald and Harbaugh, 1988) based integrated surface water – groundwater and water quality simulation model. MODHMS uses an integrated finite difference approach and is capable of modelling the interactions between surface water, groundwater, and channel flow domains. The 3-dimensional variably saturated groundwater flow is calculated using the Richard's equation, while the overland flow is calculated using a diffusion wave approximation of the St. Venant equation. Flow through 1-dimensional channels is calculated using the diffusion wave approximation with the Priesmann Slot conceptualization for pressurized flow in pipes. MODHMS incorporates an evapotranspiration module along with the surface water and groundwater flow modules to account for all components of the hydrologic cycle. (HydroGeoLogic, 2005)

This fully-integrated model solves the overland, vadose zone, groundwater, and channel flows simultaneously for each timestep. This fully-integrated, fully-coupled solution accurately simulates all dominant hydrologic processes, while a sequential flow coupling option is incorporated and can provide fast and efficient solutions to systems with weak surface water – groundwater interactions. (HydroGeoLogic, 2005)

2.2.4 HydroGeoSphere

HydroGeoSphere (Therrien et al., 2005) is a Frac3DVS based integrated surface water – groundwater flow simulation model based on the work by VanderKwaak (1999). HydroGeoSphere can use both an integrated finite difference or an integrated finite element approach and is capable of modelling the interactions between surface water, groundwater, and channel flow domains. HydroGeoSphere also offers the option of dual

continua (fractured flow) groundwater flow simulation. The 3-dimensional variably saturated groundwater flow component is calculated using a modified form of Richard's equation. The overland flow and channel flow domains are calculated similar to MODHMS, using a diffusion wave approximation of the St. Venant equation along with the Manning equation for overland flow. HydroGeoSphere also accounts for evapotranspiration in much the same fashion as does MODHMS. This fully-integrated model solves the overland, vadose zone, groundwater, and channel flows simultaneously for each timestep. (Therrien et al., 2005)

HydroGeoSphere and all of its theoretical background will be further discussed in Chapter 3.

Chapter 3

Development of Integrated Surface Water – Groundwater Flow Equations

The development of the theoretical equations used by the HydroGeoSphere model (Therrien et al., 2005) are discussed in this chapter. This theoretical evaluation presents the equations of groundwater and surface water flow, with specific attention being paid to the linkage term and the evapotranspiration component of the HydroGeoSphere simulator.

3.1 GROUNDWATER FLOW

The variably saturated groundwater component, for a single continuum subsurface (porous medium), is described by a modified version of the three-dimensional Richards equation. Four primary assumptions are made for the subsurface flow: the fluid is incompressible, the porous medium is non-deformable, the system is under isothermal conditions, and the air phase is infinitely mobile (Therrien et al, 2005). Unless otherwise

noted, the defining groundwater equations are taken or expanded from Therrien et al. (2005).

The modified version of the Richards' equation is defined by

$$-\left[\frac{\partial q_x}{\partial x}+\frac{\partial q_y}{\partial y}+\frac{\partial q_z}{\partial z}\right]+\sum \Gamma_{ex} \pm Q=\frac{\partial}{\partial t}(\theta_s S_w) \tag{3.1}$$

where the fluid flux components (L T^{-1}), q_x, q_y, and q_z, are defined by

$$q_x=-K_{xx}\cdot k_r\frac{\partial(\psi+z)}{\partial x} \tag{3.2}$$

$$q_y=-K_{yy}\cdot k_r\frac{\partial(\psi+z)}{\partial y} \tag{3.3}$$

$$q_z=-K_{zz}\cdot k_r\frac{\partial(\psi+z)}{\partial z} \tag{3.4}$$

where K_{**} is the hydraulic conductivity in the ** direction (L T^{-1}), k_r is the relative permeability of the medium (-), Ψ is the pressure head (L), and z is the elevation head (L).

The hydraulic conductivity of the porous medium is defined by Freeze and Cherry (1979) as

$$K=\frac{\rho g k}{\mu} \tag{3.5}$$

where ρ is the density of water (M L^{-3}), g is the gravitational acceleration experienced by the water (L T^{-2}), μ is the viscosity of the water (M L^{-1} T^{-1}), and k is the permeability of the porous medium (L^2). $\Sigma\Gamma_{ex}$ is the fluid exchange flux (L^3 L^{-3} T^{-1}) between the surface

and subsurface flow regimes, where a positive value represents a flow into the subsurface. Q is defined as a source (+ve) or a sink (-ve) flux within the subsurface.

The storage term of the modified Richards equation is approximated with the following relationship (Cooley, 1971 & Neuman, 1973):

$$\frac{\partial}{\partial t}(\theta_s S_w) \approx S_w S_s \frac{\partial \psi}{\partial t} + \theta_s \frac{\partial S_w}{\partial t} \tag{3.6}$$

where θ_s is the saturated water content (-), S_w is the water saturation (-), and S_s is the specific storage coefficient of the porous medium (L^{-1}).

3.2 SURFACE WATER FLOW

The surface water component of HydroGeoSphere is calculated with a two-dimensional diffusion wave approximation of the St. Venant equations. This approximation makes several assumptions originating from the St. Venant equations: inertial terms are neglected, depth-averaged flow velocities are used, the vertical pressure distribution is hydrostatic, only mild slopes are considered, and bottom shear stresses are dominant. Unless otherwise noted, the defining surface water equations are taken or expanded from Therrien et al. (2005).

The three components of the two-dimensional St. Venant equations for unsteady shallow water flow include the mass balance equation:

$$\frac{\partial \phi_o h_o}{\partial t} + \frac{\partial \left(\bar{v}_{xo} d_o\right)}{\partial x} + \frac{\partial \left(\bar{v}_{yo} d_o\right)}{\partial y} + d_o \Gamma_o \pm Q_o = 0 \tag{3.7}$$

the momentum equation for the x-direction:

$$\frac{\partial}{\partial t}\left(\bar{v}_{xo} d_o\right) + \frac{\partial}{\partial x}\left(\bar{v}_{xo}^2 d_o\right) + \frac{\partial}{\partial y}\left(\bar{v}_{xo} \bar{v}_{yo} d_o\right) + g\, d_o \frac{\partial d_o}{\partial x} = g\, d_o \left(S_{ox} - S_{fx}\right) \tag{3.8}$$

and the momentum equation for the y-direction:

$$\frac{\partial}{\partial t}\left(\bar{v}_{yo} d_o\right) + \frac{\partial}{\partial x}\left(\bar{v}_{yo}^2 d_o\right) + \frac{\partial}{\partial y}\left(\bar{v}_{xo} \bar{v}_{yo} d_o\right) + g\, d_o \frac{\partial d_o}{\partial x} = g\, d_o \left(S_{oy} - S_{fy}\right) \tag{3.9}$$

where d_o is the depth of surface water flow (L), z_o is the ground surface elevation (L), h_o is the water surface elevation (where $h_o = z_o + d_o$) (L), $\bar{v}_{xo}$ and $\bar{v}_{yo}$ are the vertically averaged flow velocities in the x and y directions (L T^{-1}), Q_o is a volumetric flow rate per unit area representing external sources and sinks (L T^{-1}), g is gravitational acceleration (L T^{-2}), ϕ_o is a surface flow domain porosity equal to unity over flat surfaces and varying from zero to unity over uneven surfaces, and Γ_o is the fluid flow from the subsurface to the surface system.

Variables S_{ox} and S_{oy} are the bed slopes in the x- and y- directions (-) while S_{fx} and S_{fy} represent the friction slopes in the x- and y- directions (-). The friction slopes are further defined using the Manning equation as:

$$S_{fx} = \frac{\bar{v}_{xo} \bar{v}_{so} n_x^2}{d_o^{4/3}} \tag{3.10}$$

and

$$S_{fy} = \frac{\bar{v}_{yo} \bar{v}_{so} n_y^2}{d_o^{4/3}} \tag{3.11}$$

where n_x and n_y are the Manning roughness coefficients in the x- and y- directions ($L^{-1/3}$ T), and $\bar{v}_{so}$ is the vertically averaged flow velocity along the maximum slope (L T^{-1}).

The surface conductances K_{ox} and K_{oy} (L T^{-1}), using the Manning equation, are defined by:

$$K_{ox} = \frac{d_o^{2/3}}{n_x} \frac{1}{[\partial h_o / \partial s]^{1/2}} \tag{3.12}$$

and

$$K_{oy} = \frac{d_o^{2/3}}{n_y} \frac{1}{[\partial h_o / \partial s]^{1/2}} \tag{3.13}$$

where the slope, s, is the direction of maximum slope (-).

The resulting diffusion wave approximation solved by HydroGeoSphere is expressed as:

$$\frac{\partial \phi_o h_o}{\partial t} - \frac{\partial}{\partial x}\left(d_o K_{ox} \frac{\partial h_o}{\partial x} \right) - \frac{\partial}{\partial y}\left(d_o K_{oy} \frac{\partial h_o}{\partial y} \right) + d_o \Gamma_o \pm Q_o = 0 \tag{3.14}$$

3.3 GROUNDWATER – SURFACE WATER LINKAGE METHOD

Within the HydroGeoSphere code, two different approaches exist by which the water exchange terms, Γ_{ex}, can be calculated. These approaches are referred to as common node and dual node linkage schemes. Unless otherwise noted, the defining surface – subsurface linkage theory and equations are taken from Therrien et al. (2005).

The common node linkage scheme is based on the assumption of hydraulic head continuity between the two flow domains (surface and subsurface). As pressure

equilibrium exists between the two domains, the calculation of the fluid flux between the two systems is calculated post time step during post-processing.

The dual node linkage scheme does not assume continuity of hydraulic head between the two flow domains. The head difference is treated as the driving force in determining the fluid flux between the two domains. This method assumes a thin layer of porous material between the surface and subsurface across which the fluid flux occurs. The head difference between the layers and the resistance to flow (leakance) of the thin porous medium are two of the controlling parameters for the fluid exchange.

The subsurface of the Bass Lake domain is modelled using an assumed equivalent porous medium without considering additional major fractures, macropores, or injection/extraction wells. The reasoning behind this representation is further discussed in Section 5.4. The single continuum surface – subsurface linkage term is:

$$d_o \Gamma_o = k_{ro} K_{so} \left(h - h_o \right) \tag{3.15}$$

where d_o and Γ_o are defined in the surface water flow equations, k_{ro} accounts for the rill storage effects (-), K_{so} is the leakance factor across the thin porous medium layer (T^{-1}), h is the subsurface head (L), and h_o is the surface head (L).

The leakance factor, K_{so}, can be further defined as

$$K_{so} = \frac{K}{\Delta T} \tag{3.16}$$

where K is the hydraulic conductivity of the thin porous medium (L T^{-1}) and ΔT is the thickness through which the fluid flux occurs (L).

3.4 EVAPOTRANSPIRATION

The evapotranspiration component of HydroGeoSphere is simulated using the "bucket model" as detailed by Panday and Huyakorn (2004). The bucket model functions such that any precipitation in excess of interception storage and evaporation from interception reaches the ground surface. Interception is the process defined as the amount of precipitation remaining on any part of the vegetative cover above the ground surface. The interception storage can vary from zero to the interception storage capacity, $S_{\text{int}}^{\max}$. The interception storage capacity (L) is a function of the vegetation type and the growth stage of the vegetation and is defined by (Panday and Huyakorn, 2004):

$$S_{\text{int}}^{\max} = c_{\text{int}} LAI \tag{3.17}$$

where c_{int} is the canopy storage parameter (L) and LAI is the leaf area index (-).

The actual interception storage, S_{int}, is calculated for each time step (Δt) and is defined by:

$$S_{\text{int}} = S_{\text{int}}^{*} - E_{can} \cdot \Delta t \tag{3.18}$$

where

$$S_{\text{int}}^{*} = \min(S_{\text{int}}^{\max}, S_{\text{int}}^{0} + P_p \cdot \Delta t) \tag{3.19}$$

and

$$E_{can} \cdot \Delta t = \min(S_{\text{int}}^{*}, E_p \cdot \Delta t) \tag{3.20}$$

The variables S_{int}^{0} and S_{int}^{*} are the previous and intermediate time values of S_{int}, P_p is the precipitation rate (L T^{-1}), E_{can} is the canopy evaporation (L T^{-1}), and E_p is the reference evapotranspiration (L T^{-1}) (further detailed in Section 5.6.4).

The rainfall reaching ground surface, $\widehat{P}_p$ is defined by:

$$\widehat{P}_p = P_p - (S_{\text{int}} - S_{\text{int}}^0)/\Delta t - E_{can} \geq 0 \tag{3.21}$$

The evapotranspiration is modelled with evaporation and transpiration components affecting surface and subsurface nodes. All vegetative transpiration occurs from the ground surface to the maximum vegetative root depth and can encompass multiple subsurface layers. The transpiration rate for node *i* (T_{pi}) is defined as:

$$T_{pi} = [f_1(LAI)][f_2(\theta_i)][RDF_i][E_p - E_{can}] \tag{3.22}$$

where $f_1(LAI)$ is a function of the leaf area index and is defined by;

$$f_1(LAI) = \max\{0, \min[1, (C_2 + C_1 \cdot LAI)]\} \tag{3.23}$$

$f_2(\theta_i)$ is a function of nodal water content expressed as

$$f_2(\theta_i) = \begin{cases} 0 & for\ 0 \leq \theta_i \leq \theta_{wp} \\ 1 - \left[\dfrac{\theta_{fc} - \theta_i}{\theta_{fc} - \theta_{wp}}\right]^{c_3/E_p} & for\ \theta_{wp} < \theta_i \leq \theta_{fc} \\ 1 & for\ \theta_{fc} < \theta_i \leq \theta_o \\ \left[\dfrac{\theta_{an} - \theta_i}{\theta_{an} - \theta_o}\right]^{c_3/E_p} & for\ \theta_0 < \theta_i \leq \theta_{an} \\ 0 & for\ \theta_{an} \leq \theta_i \end{cases} \tag{3.24}$$

and RDF_i is defined by

$$RDF_i = \int_{z_1}^{z_2} r_f(z)\, dz \Big/ \int_{0}^{L_1} r_f(z)\, dz \tag{3.25}$$

where C_1, C_2 and C_3/E_p are fitting parameters (-), θ_{wp}, θ_{fc}, θ_o, and θ_{an} are the moisture contents at the wilting point, field capacity, oxic limit, and anoxic limits (-), L_r is the effective root length (L), $r_f(z)$ is the root extraction function (depth varying).

The root distribution function, *RDF*, should be assigned such that the following constraint holds true for each vertical set of nodes:

$$RDF = \sum_{i=1}^{n_R} RDF_i = 1 \tag{3.26}$$

where n_R is the total number of nodes found within the root zone for the given x – y location.

Two different models are used to calculate the evaporation (E_{si}). The first model assumes that evaporation occurs if the sum of the canopy evaporation and plant transpiration are less than the reference evapotranspiration. The resulting evaporation from the surface and subsurface layers is calculated by

$$E_{s_i} = \left[\alpha_i^*\right]\left[E_p - E_{can} - T_p\right]\left[EDF_i\right] \tag{3.27}$$

The second model is defined by

$$E_{s_i} = \left[\alpha_i^*\right]\left[E_p - E_{can}\right]\left[1 - f_1(LAI)\right]\left[EDF_i\right] \tag{3.28}$$

where the wetness factor, α_i^*, is given by

$$\alpha_i^* = \begin{cases} (\theta_i - \theta_{e2})/(\theta_{e1} - \theta_{e2}) & for\ \theta_{e2} \le \theta \le \theta_{e1} \\ 1 & for\ \theta_i > \theta_{e1} \\ 0 & for\ \theta_i < \theta_{e2} \end{cases} \tag{3.29}$$

The variable θ_{e1} is the moisture content at the end of the energy-limiting stage (-) and θ_{e2} is the limiting moisture content (-). The evaporation distribution function, *EDF*, is applied to a group of vertical nodes in both the surface and subsurface flow domains. The two models differ in that the first model assumes that the capacity for evaporation decreases with depth from the surface, whereas the second model has an evaporation capacity that extends from the surface to a prescribed extinction depth.

3.5 SURFACE WATER EVAPORATION

The surface water evaporation component of the evapotranspiration processes occurring in nature can account for the losses greater than 30 percent of the precipitation falling within climates such as those affecting the Bass Lake watershed. To account for the losses due to evaporation, a combined mass-transfer/energy balance method was used. This method, modified from Vardavas (1987) uses the Penman (1948) equation (3.30) and calculates the evaporative losses due to both the net solar radiation and the losses due to wind effects, assuming a free-water surface and no heat advection or storage. The evaporative losses, E (mm/day), can be determined with

$$E = \frac{\Delta}{\Delta + \gamma} E_s + \frac{\gamma}{\Delta + \gamma} E_a \tag{3.30}$$

where E_s is the evaporation from solar heating (mm/day), E_a is the evaporation resulting from wind and vapour pressure difference (mm/day), Δ is the slope of the vapour pressure-temperature relation (mbar/^{o}K), and γ is the psychrometric constant (mbar/^{o}K).

The slope of the vapour pressure-temperature relation (Δ) is defined by

$$\Delta = \frac{e_s - e_z}{T_s - T_z} \tag{3.31}$$

where T_s is the average daily water surface temperature (^{o}K), T_z is the average daily dry bulb air temperature (^{o}K), e_s is the saturation vapour pressure at T_s (mbar), and e_z is the saturation vapour pressure at T_s (mbar).

The psychrometric constant (γ) is defined by (Brutsaert, 1984)

$$\gamma = \frac{c_p \cdot p \cdot M_d}{L \cdot M_v} \tag{3.32}$$

where c_p is the specific heat of air (0.24 cal g^{-1} ^{o}K^{-1}), p is the average daily atmospheric pressure (mbar), M_d and M_v are the mean molecular weights of dry air and water vapour (M_v/M_d = 0.622), and L is the specific heat of vaporization of water (cal/g) given by:

$$L = 597.3 - 0.553(T_s - T_o) \tag{3.33}$$

where T_o = 273.15 ^{o}K.

3.5.1 Evaporation From Solar Heating (E_s)

Evaporation from solar heating is calculated using the Energy Balance method. For a free water surface and assuming no heat advection or storage (Bras, R., 1990), the energy balance method can be simplified to

$$E_s = \frac{Q_s - Q_r + Q_a - Q_{ar} - Q_{bs}}{\rho[L(1+R)]} \cdot 14400 \tag{3.34}$$

where Q_s is the daily averaged incident solar radiation (cal cm^{-2} min^{-1}), Q_r is the daily averaged reflected solar radiation (cal cm^{-2} min^{-1}), Q_a is the daily averaged incoming longwave radiation (cal cm^{-2} min^{-1}), Q_{ar} is the daily averaged reflected longwave radiation (cal cm^{-2} min^{-1}), Q_{bs} is the daily averaged longwave radiation emitted by a water body (cal cm^{-2} min^{-1}), ρ is the density of water (g/cm^3), and R is the Bowen Ratio (unitless).

Q_r is a function of Q_s and the estimated albedo determined from Figure 3.5.1.

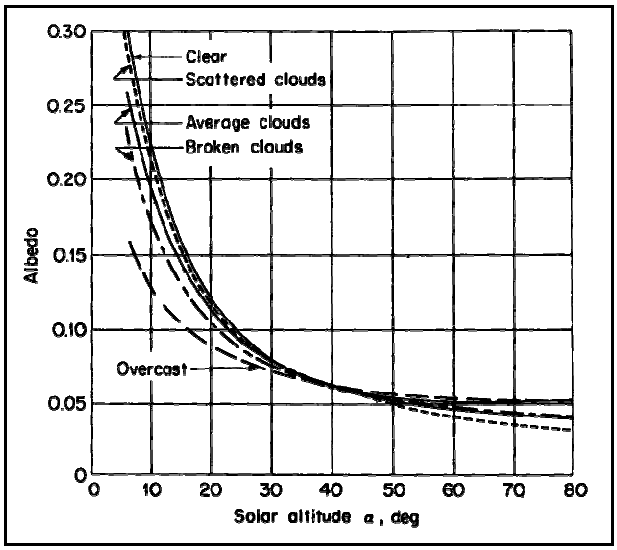

Figure 3.5.1 – Estimated Albedo (Bras, 1990)

The longwave radiation term is calculated by first determining the atmospheric emissivitiy (E_a) using equation (3.35)

$$E_a = 0.740 + 0.0049 e_z \tag{3.35}$$

Given the longwave albedo of water is approximately 0.03, the net incoming longwave radiation can be estimated using the following relationship

$$Q_a - Q_{ar} = 0.97 \cdot E_a \cdot \sigma \cdot T_z^4 \tag{3.36}$$

where $\sigma = 0.826 \times 10^{-10}$ cal cm^{-2} min^{-1} ^{o}K^{-4}.

As water radiates as a black body, Q_{bs} is calculated with:

$$Q_{bs} = \sigma \left(T_s\right)^4 \tag{3.37}$$

The Bowen Ratio, R, is the ratio of energy available for sensible heating to energy available for latent heating and is given by

$$R = \left(0.61 \times 10^{-3} \cdot p\right) \frac{\left(T_s - T_z\right)}{\left(e_s - e_z\right)} \tag{3.38}$$

3.5.2 Evaporation from Wind and Vapour Pressure Difference (E_a)

The contribution of wind and vapour pressure difference was determined by Penman (1948) and is represented by

$$E_a = f(\overline{u})\left(e_s - e_z\right) \tag{3.39}$$

This relationship was reduced and used by Vardavas (1987) as

$$E_a = C_w \cdot \overline{u} \cdot (1 - r_H) \cdot e_s \tag{3.40}$$

where $\overline{u}$ is the average daily windspeed (m/s), r_H is the daily average relative humidity as a fraction, and C_w is defined by

$$C_w = \frac{3966}{T_a \cdot \ln \frac{z_2}{z_{0v}} \cdot \ln \frac{z_1}{z_{0m}}} \tag{3.41}$$

where z_2 is the height of the water vapour pressure measurement (m), z_1 is the height of the wind speed measurement (m), and z_{0v} (m) and z_{0m} (m) are defined by

$$z_{0v} = \frac{0.135v}{u_*} \tag{3.42}$$

$$z_{0m} = \frac{0.624v}{u_*} \tag{3.43}$$

where v (m^2/s) and u_* can be determined using the following

$$v = \frac{2.964 \times 10^{-6} \cdot T_a^{3/2}}{p} \tag{3.44}$$

$$\overline{u} = \frac{u_*}{k} \cdot \ln \frac{z_2 \cdot u_*}{0.135v} \tag{3.45}$$

where k is the Von Kármán constant and is taken to be 0.421 (McKeon, 2004).

3.5.3 Incoming Shortwave Radiation Calculation (Q_r)

The incoming shortwave radiation within Bass Lake watershed was determined using a theoretical approach as no site specific radiation data was available. Given the latitude and longitude for the center of the watershed (45° 06' N, 79° 41' W) and the Julian day (D), the solar altitude α (degrees) was calculated in hourly intervals. This information was then used to calculate the incoming solar radiation using the following method (Bras, 1990).

The effective solar radiation intensity, or insolation, (cal cm^{-2} min^{-1}) can be calculated using

$$I_o = \frac{W_o}{r^2} \cdot \sin\alpha \tag{3.46}$$

where W_o is the solar constant, r is the ratio of actual to mean earth-sun distance and is calculated with

$$r = 1.0 + 0.017 \cdot \cos\frac{2\pi}{365}(186 - D) \tag{3.47}$$

The clear sky shortwave radiation, I_c, is then calculated using

$$\frac{I_c}{I_o} = \exp(-n \cdot a_1 \cdot m) \tag{3.48}$$

where n is a turbidity factor of air (n = 2 for Bass Lake location) (unitless), m is the optical air mass (unitless), and a_1 is the molecular scattering coefficient defined by

$$a_1 = 0.128 - 0.054 \log_{10} m$$

(3.49)

and m is defined by

$$m = \frac{1}{\sin \alpha}$$

(3.50)

The incoming shortwave radiation, Q_r, is then defined as a function of the cloud opacity fraction (N) and I_c.

$$\frac{Q_r}{I_c} = 1 - 0.65 N^2$$

(3.51)

Chapter 4

Bass Lake Information, Background, and Conceptual Model Construction

The Bass Lake study site is located on the Precambrian Shield in the Muskoka Region of Ontario. This area is situated northwest of Toronto, bounded by Algonquin Park to the east and Georgian Bay to the west (Figure 4.0.1).

The fractured nature of the bedrock within the study site is characteristic of a Canadian Shield environment and includes numerous lakes, wetlands, and dense pine/oak/maple/birch forests. The quality of surface water and groundwater are a concern within this region as it is a frequented vacation destination. The maintenance of existing water quality levels is a major focus of Muskoka area municipalities.

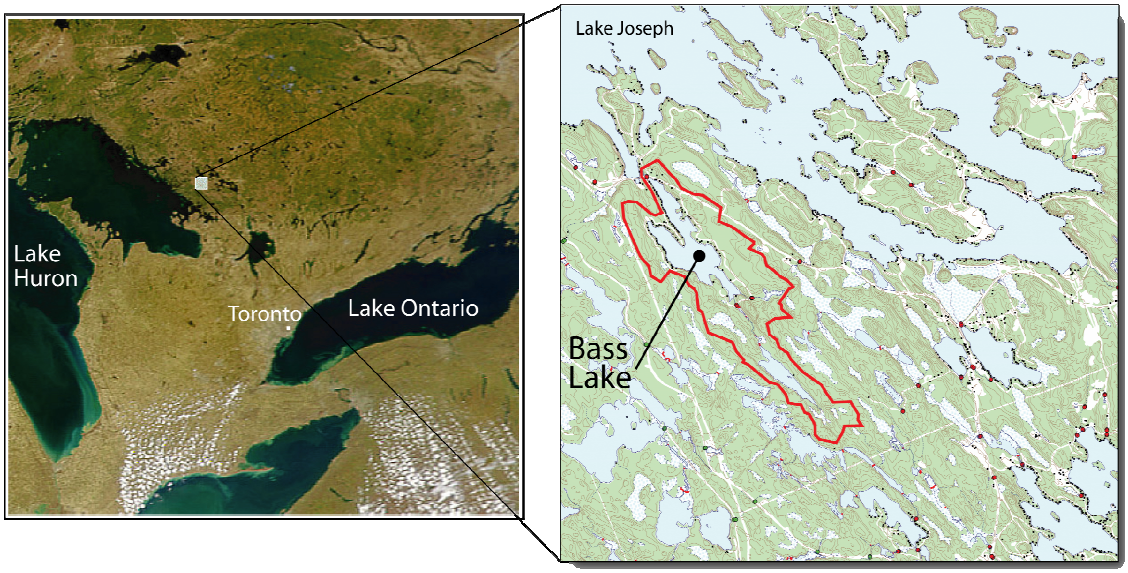

Figure 4.0.1 – Bass Lake Location (from NASA, 2004)

4.1 Site Selection and Location

With increased social awareness of the interconnectedness of groundwater and surface waters (especially in fractured bedrock systems), increasing efforts have been made to identify and quantify fluid flux between the two systems (Oxtobee, 2002). The selection of a study site to test seasonally varying flow at a watershed-scale with the numerical simulation model HydroGeoSphere was based on four main factors: the size of the study site, the geologic setting, the availability of environmental data, and the cooperativeness of area residents. The Bass Lake watershed covers a small surface area, is located on fractured crystalline bedrock, is known to have available historical precipitation and lake level data, and has area residents who expressed excitement and willingness to help wherever possible.

Bass Lake proper is located in the Township of Muskoka Lakes, west of the village of Glen Orchard, and south of Muskoka Road 169. A bathymetric survey of the lake was completed in October 2003 revealing a mean water depth of 4.5 meters and a maximum depth of 9.0 meters (DMM, 2001) (Turner, 2004). The collected bathymetric data will be further discussed in Chapter 4.3.1.

The Bass Lake watershed outflows at the north end of Bass Lake into Lake Joseph. The outflow is controlled by a natural rock weir (Chapter 4.3.2). The resulting outflows can vary from high early spring thaw flow rates to zero outflow conditions during hot and dry summer conditions.

The model domain selected, which includes the Bass Lake watershed, has a surface area of 17.7 km^2 (Figure 4.1.1). The reasoning behind the model domain boundary definition will be discussed in Chapter 5.2.

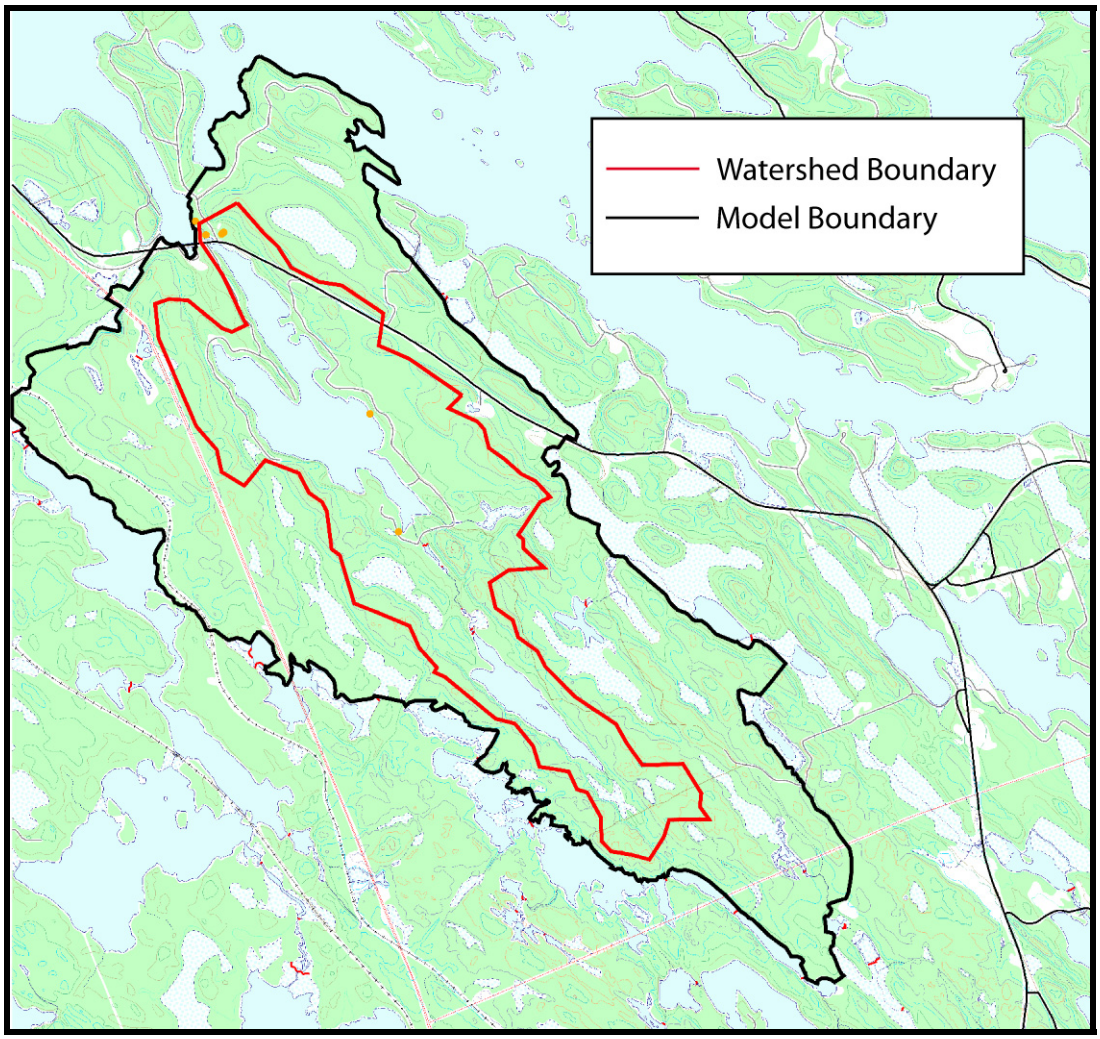

Figure 4.1.1 - Bass Lake Watershed and Model Boundaries

The Bass Lake watershed was delineated using Ontario Base Maps (OBMs) at a scale of 1:10000. The watershed has a surface area of 6.92 km^2 with two major lakes, Bass Lake (0.94 km^2) and Long Lake (0.23 km^2; also know as Concession Lake). The relief of the watershed varies widely from a minimum elevation of 216.5 m to a maximum elevation of 265.0 m.

4.2 DIGITAL ELEVATION MODEL

To create an accurate estimate of surface elevations across the model domain, a digital elevation model (DEM) was created. It was created using digital versions of OBMs. The surface contours (5 m contour interval) were used to create a surface TIN for the elevations (Figure 4.2.1). Further DEM refinement to include bathymetry and flat area corrections is discussed in Chapter 5.3.3.

4.3 FIELD DATA COLLECTION

A previous study of the Bass Lake watershed (Randall et al., 2003) collected precipitation and lake level response data from September to December 2002. Further data collection efforts were required to increase the frequency and magnitude of the climate data for locations within the watershed. These data collection efforts included conducting a bathymetric survey, a natural rock weir cross-section survey, and implementing surface soil, precipitation, and lake level data sampling programs.

4.3.1 Bathymetric Survey

To minimize much of the uncertainty associated with the DEM in submerged areas affecting the modelling domains, a bathymetric survey of Bass Lake was completed in October 2003.

The survey locations were collected with a handheld Global Positioning System (GPS) device with an accuracy of ± 3 meters. The water depths at each survey location were initially measured with a tape measure and weight. However, it was determined that water depth data collection with this method would require several days and would offer less than optimal depth accuracy (due to wind effects, sampling time, angled depth measurements, etc.). As a result, a sonar depth sounder, in the form of a commercially available fish finder, was used to collect the water depths.

A total of 1945 data points were collected around Bass Lake (Figure 4.3.1). At every 40th sampling location, a sample of water depth was collected using both depth sounder and tape sampling methods to ensure measurement accuracy. The calibration data showed an average difference of 1.2% between the sonar sounding depths and the hand measured depths.

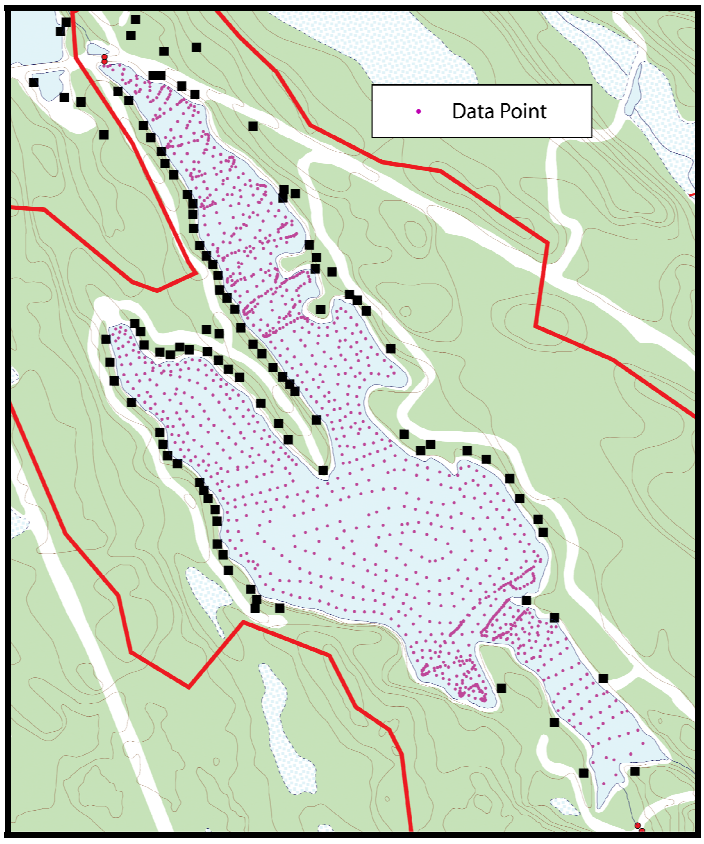

Figure 4.3.1 – Bass Lake Bathymetric Survey Data Points

The water depths were subtracted from the observed Bass Lake surface elevation to create the lake bathymetry. Similar to the DEM, the lake bottom contours were used to create a 3-dimensional surface map for Bass Lake (Figure 4.3.2).

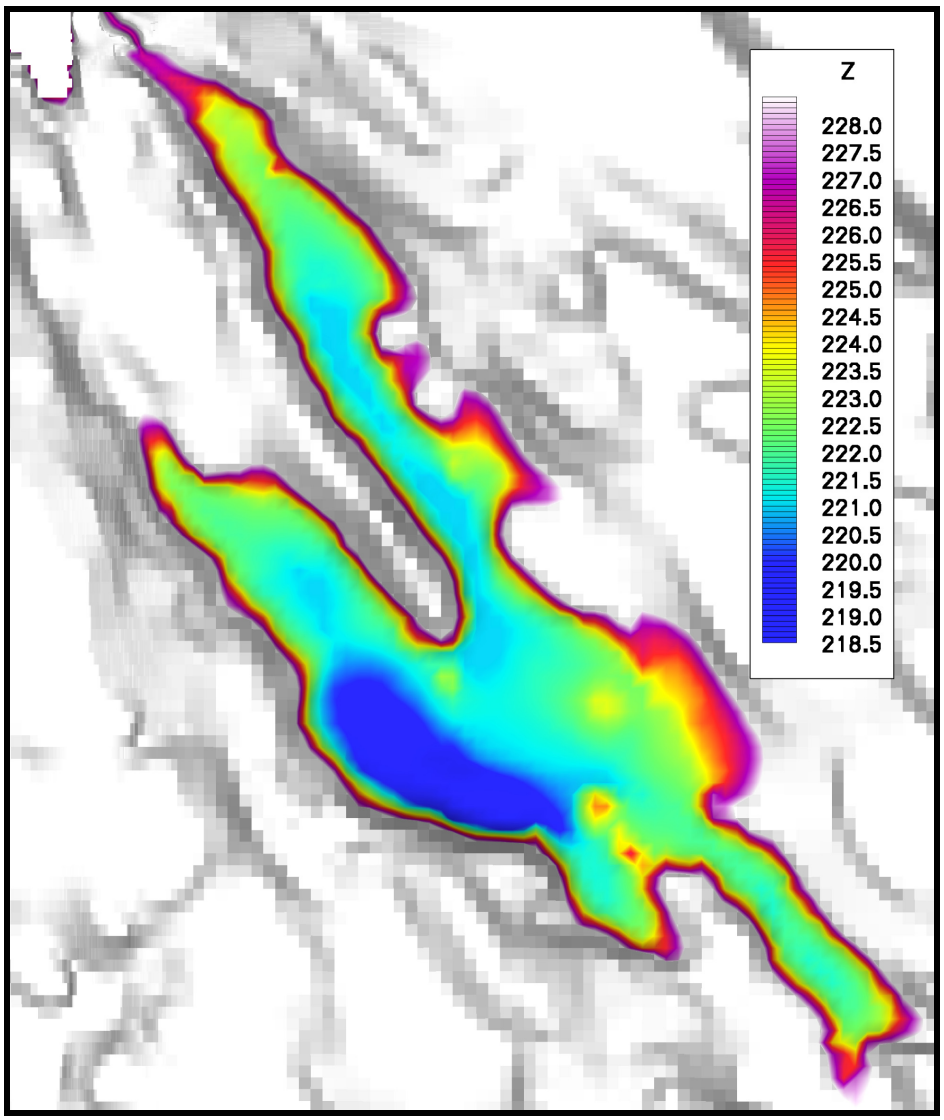

Figure 4.3.2 – Bass Lake Bottom Elevation

4.3.2 Natural Rock Weir Cross-Sectional Survey

The natural rock weir located at the north end of Bass Lake (Figure 4.3.3) provides hydraulic control for surface water outflow from the watershed (Figure 4.3.4). As a result, an accurate cross-sectional survey was completed to determine the elevations

across the weir. The surveyed elevations were referenced to Ontario Highway Benchmark 156-69 (elevation 228.890 m) (Figure 4.3.3) and the results are presented on Figure 4.3.5.

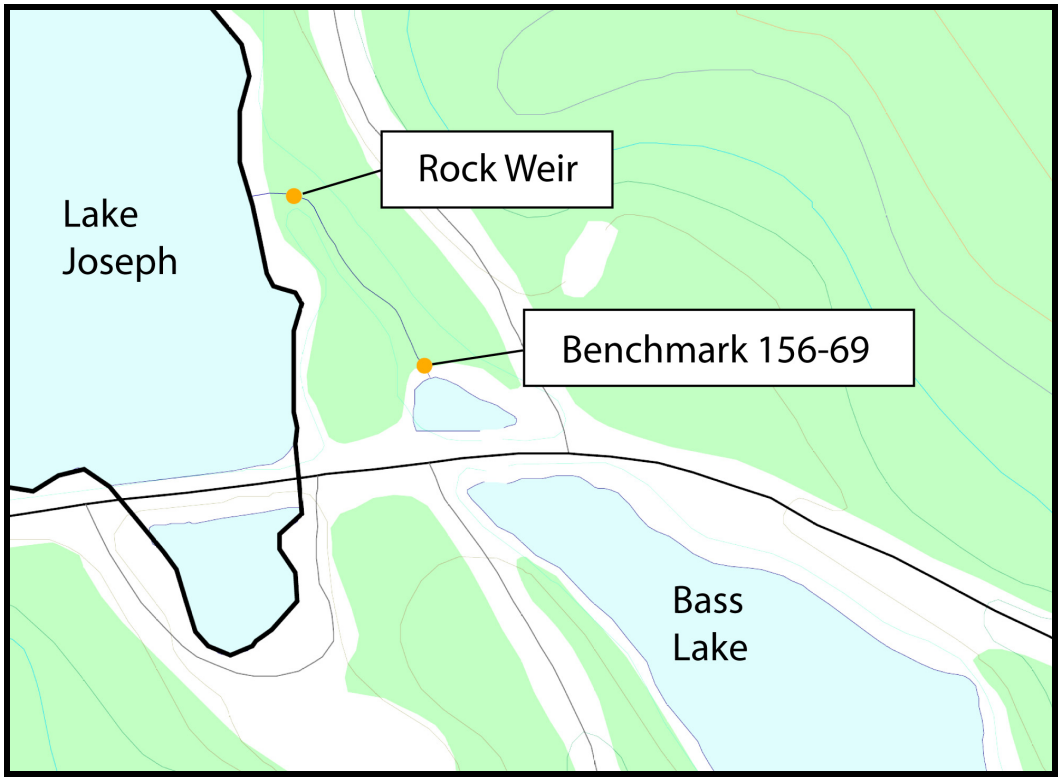

Figure 4.3.3 – Rock Weir and Ontario Highway Benchmark Location

Figure 4.3.4 – Bass Lake Rock Weir

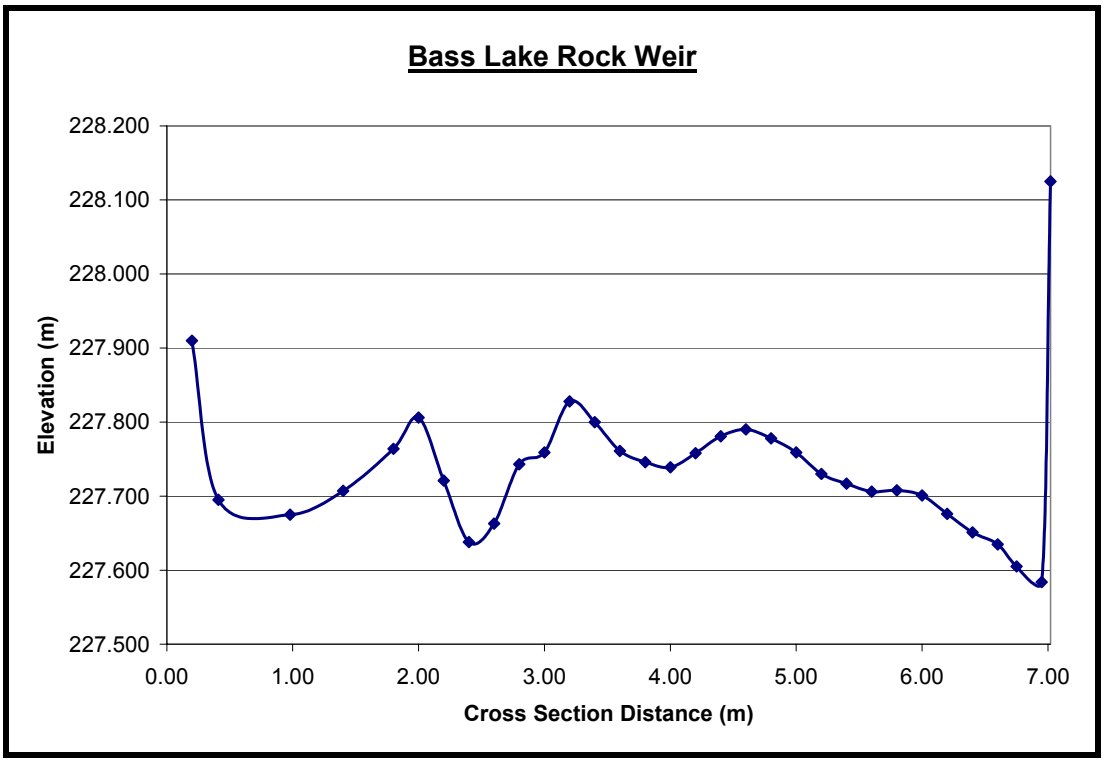

Figure 4.3.5 – Rock Weir Cross Section Elevations

4.3.3 Surficial Soil Sampling

Minimal surficial soil cover exists in and surrounding the Bass Lake watershed. To determine the surficial soil properties within the model domain, three soil samples were taken at locations across the watershed (Figure 4.3.6).

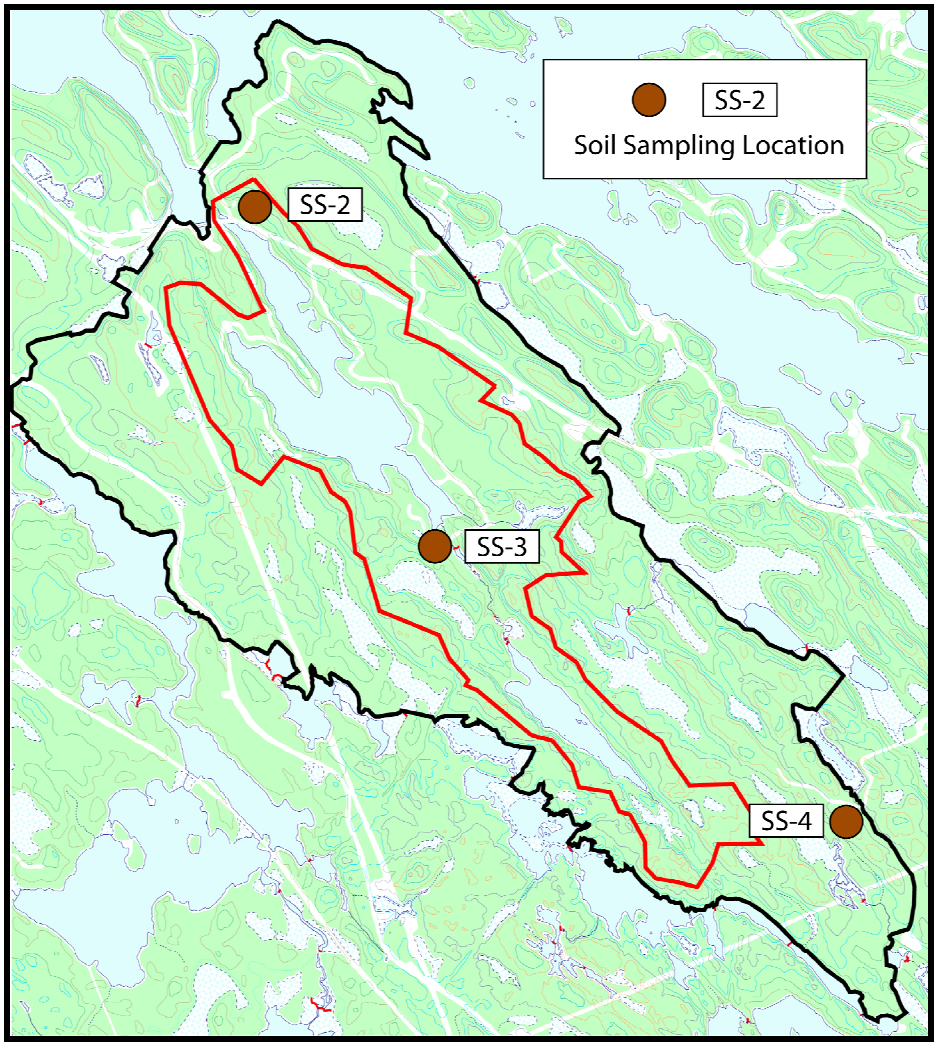

Figure 4.3.6 – Soil Sampling Locations

Grain size distribution analyses were performed on the soil samples. The results of these analyses are shown on Figure 4.3.7. From these results, it was determined that the surficial soil is a silty sand (Craig, 1997).

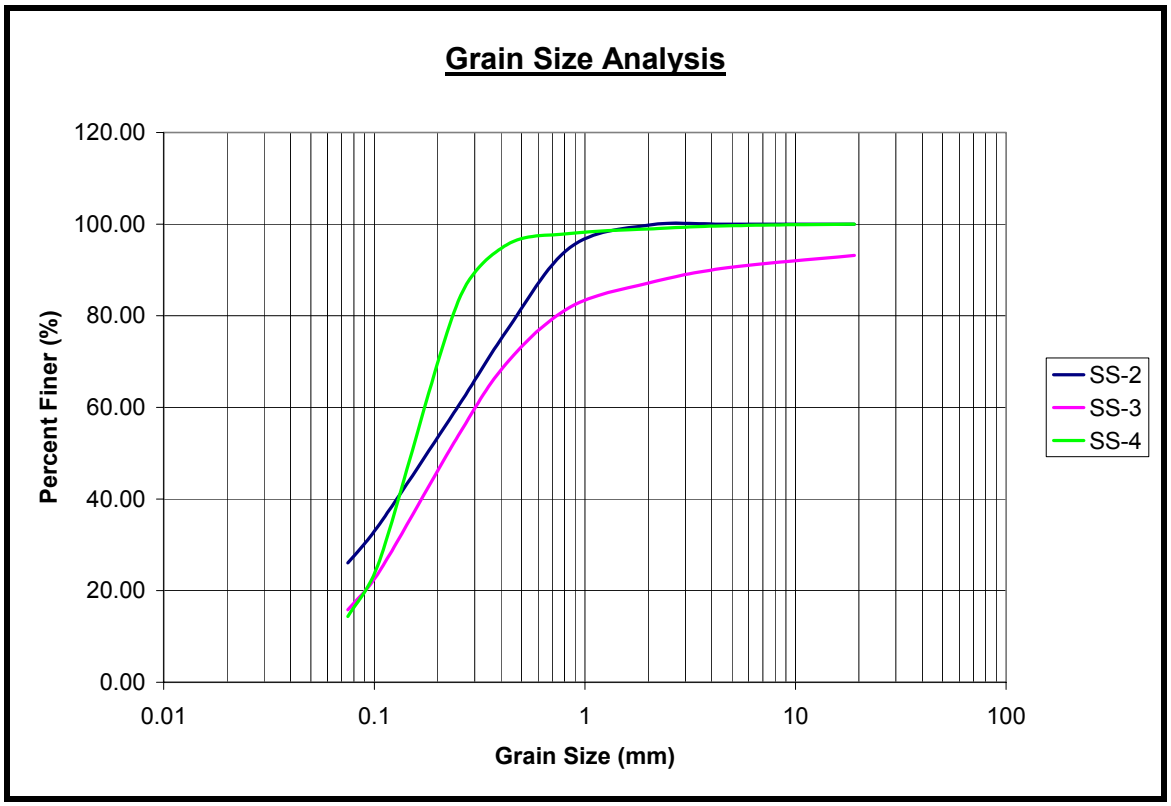

Figure 4.3.7 – Surficial Soil Grain Size Distributions

4.3.4 Precipitation Sampling Program

As the major driving force behind surface water and groundwater movements, accurate records of precipitation events allow for accurate computer simulation models. To record the precipitation within the Bass Lake model domain, three rain gauges were setup across the watershed (Figure 4.3.8).

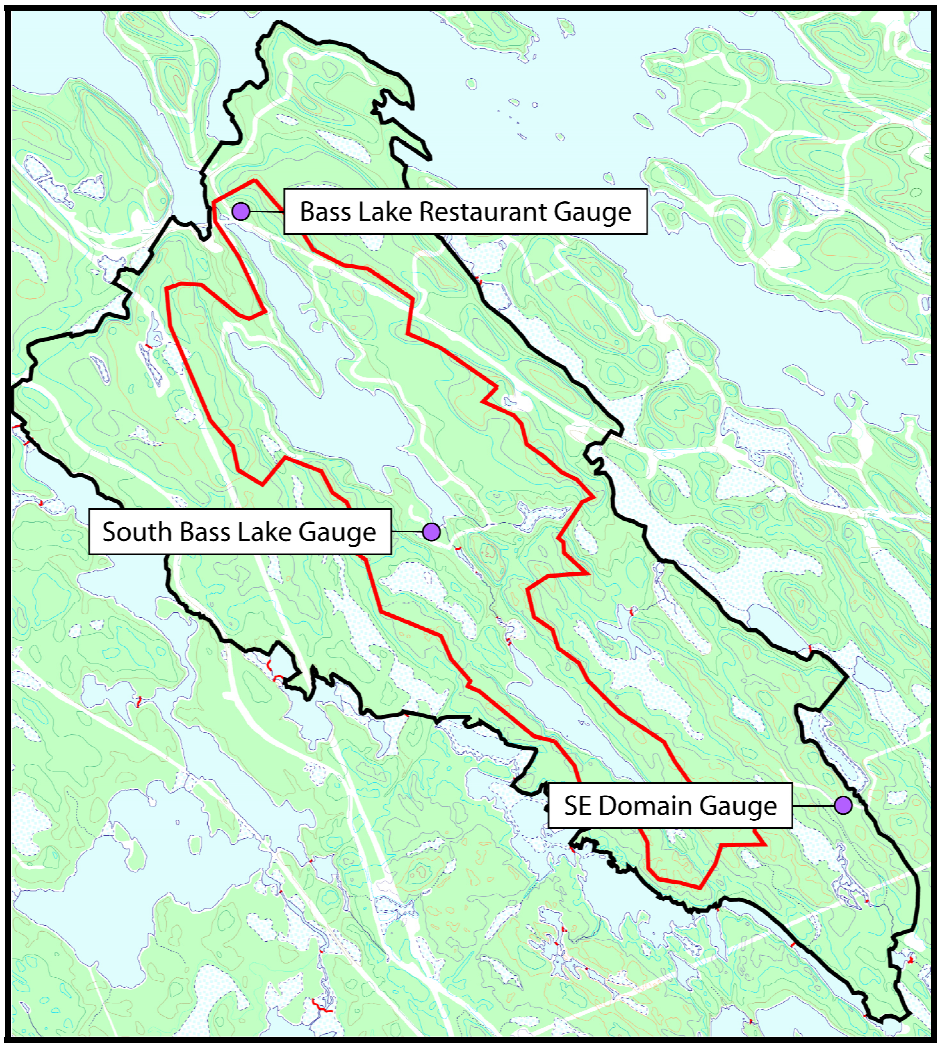

Figure 4.3.8 – Precipitation Gauge Locations

Due to animal attacks and difficult vehicular access, the SE Domain gauge was taken offline for the duration of the sampling program. The Bass Lake Restaurant gauge remained online for the majority of the sampling program; however, the data logger experienced several malfunctions resulting in periods of lost data. The South Bass Lake gauge recorded a continuous data set from April 17th to November 20th, 2004. The accumulated precipitation for the region is presented in Figure 4.3.9.

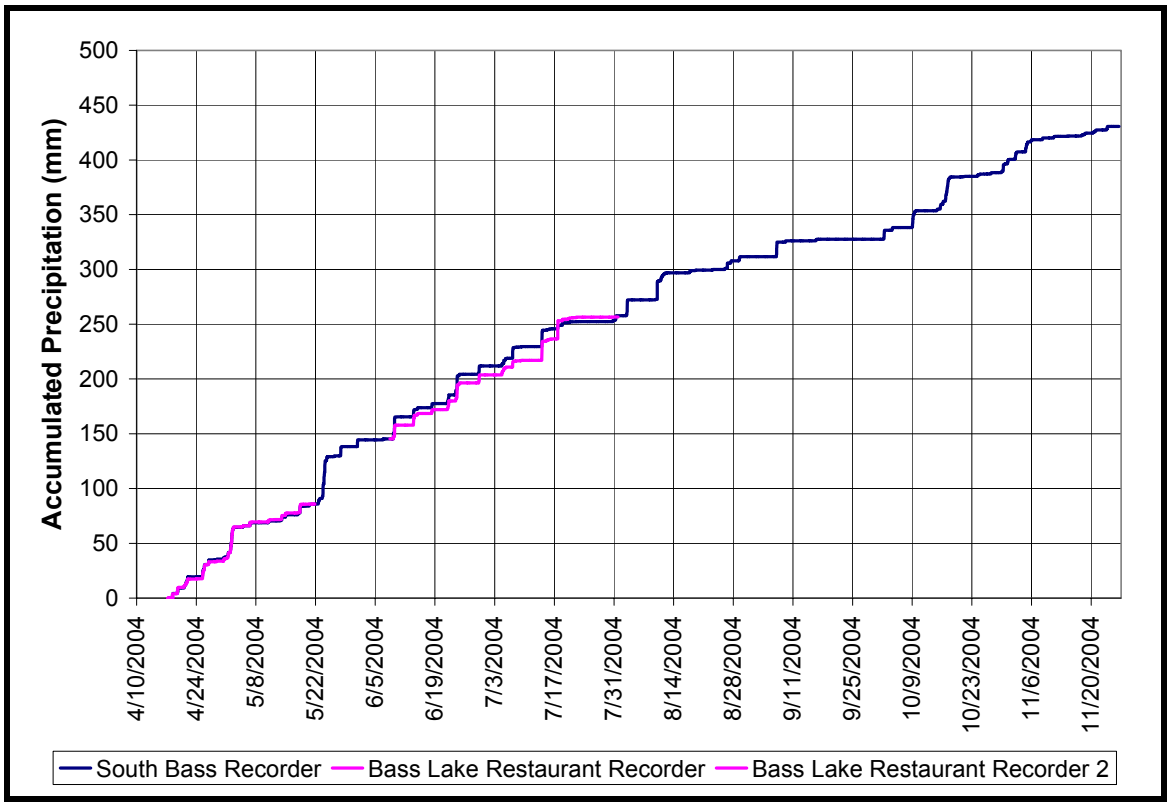

Figure 4.3.9 – Bass Lake 2004 Precipitation Data

4.3.5 Lake Level Sampling Program

With both surface water and integrated surface water-groundwater models, ensuring accurate surface water responses to precipitation events is a critical component of model calibration. With HydroGeoSphere, the fluid flux between the surface and subsurface flow regimes is described by the linkage term, which is itself controlled by the head differences between the two flow regimes. To facilitate model calibration, a lake level sampling program was designed for Bass Lake.

A pressure transducer was installed below a resident's dock on the north-east bank of Bass Lake (Figure 4.3.10), approximately 1.2 m below the water surface.

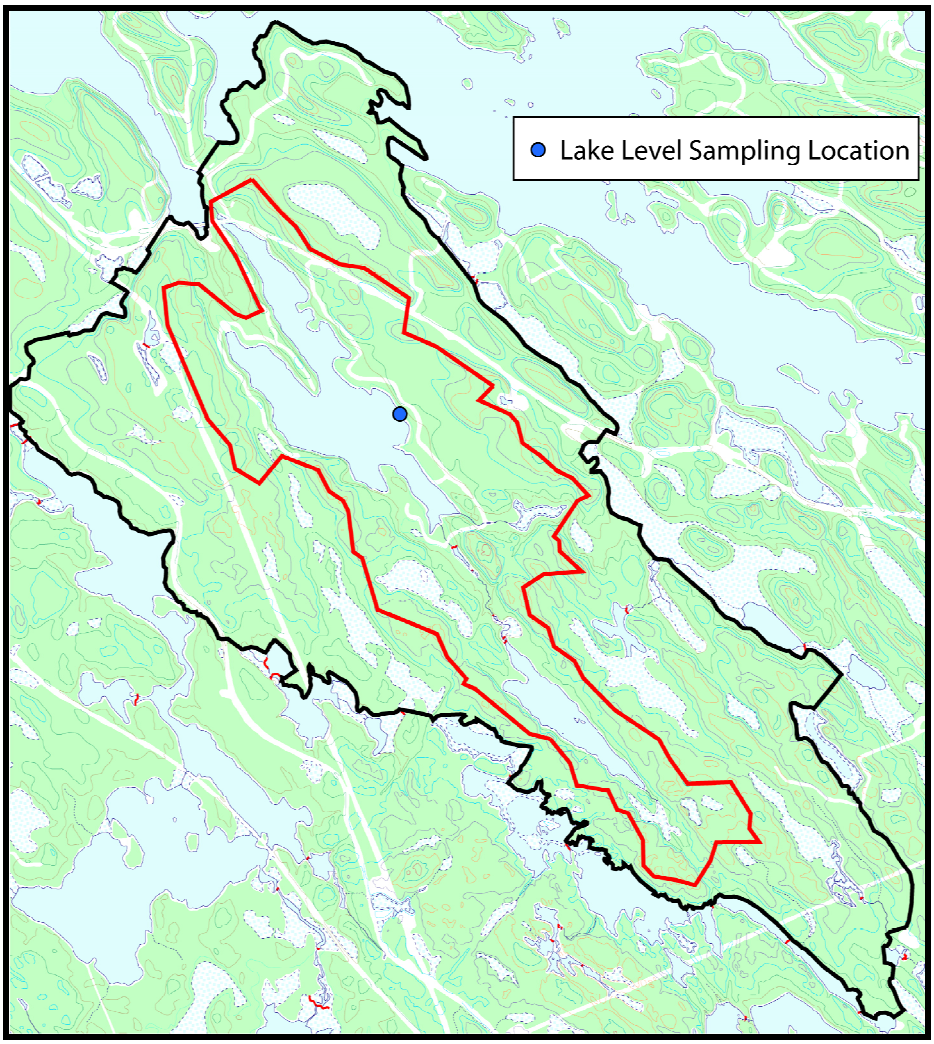

Figure 4.3.10 – Lake Level Sampling Location

Lake levels were sampled on 15 minute intervals from May 2nd to November 26th, 2004. The collected data was processed and converted the pressure reading to an equivalent depth of water, which was in turn referenced to survey data to yield the lake level elevations with respect to meters above sea level (masl). The lake levels for the sampling period are shown on Figure 4.3.11. The lake levels are displayed as one-hour moving averages (30 minutes before to 30 minutes after) in order to reduce the influence of wave action on the water surface data.

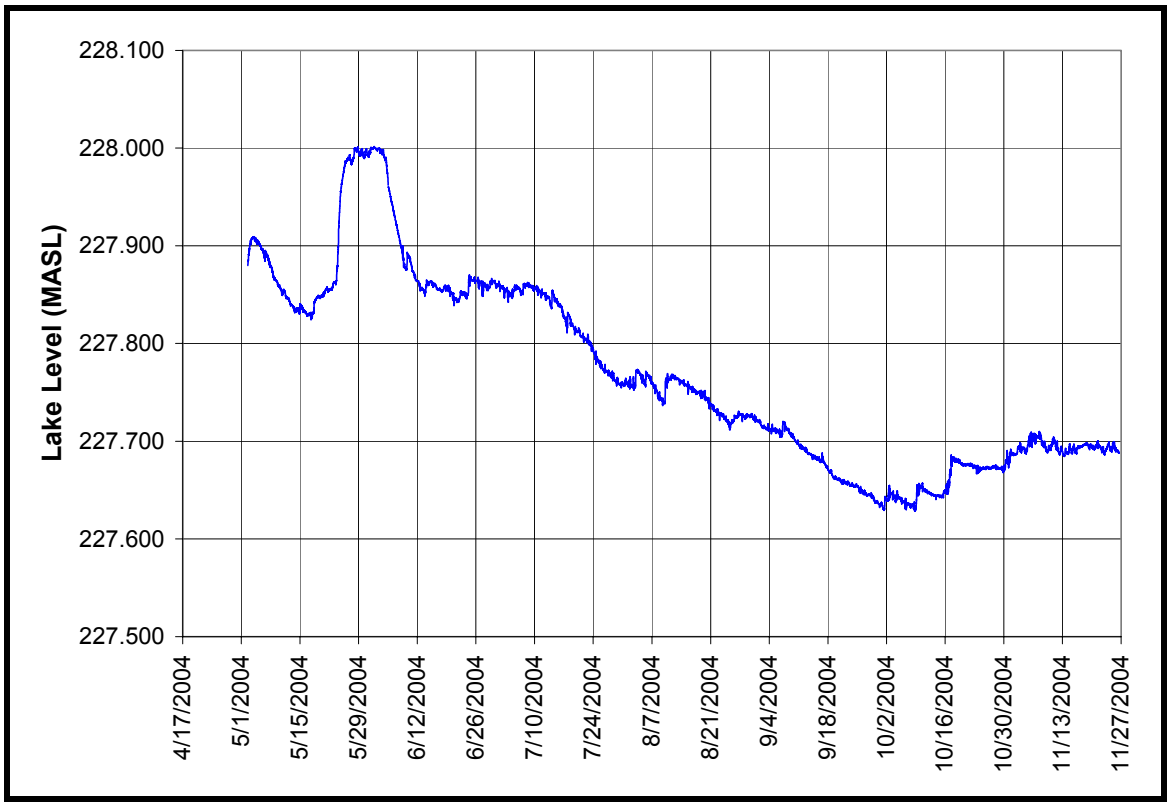

Figure 4.3.11 – Bass Lake Level

4.4 ADDITIONAL CLIMATE DATA COLLECTION

To supplement the collected precipitation and lake level data sets, additional climate data were obtained from the Canadian Ministry of Natural Resources for three weather stations within a 38 km radius of Bass Lake: Parry Sound, Muskoka Airport, and Beausoleil (Figure 4.4.1). These data sets include, but are not limited to, air temperature, relative humidity, wind speed, percentage cloud cover, and atmospheric pressure (Figures 4.4.2 to 4.4.6).

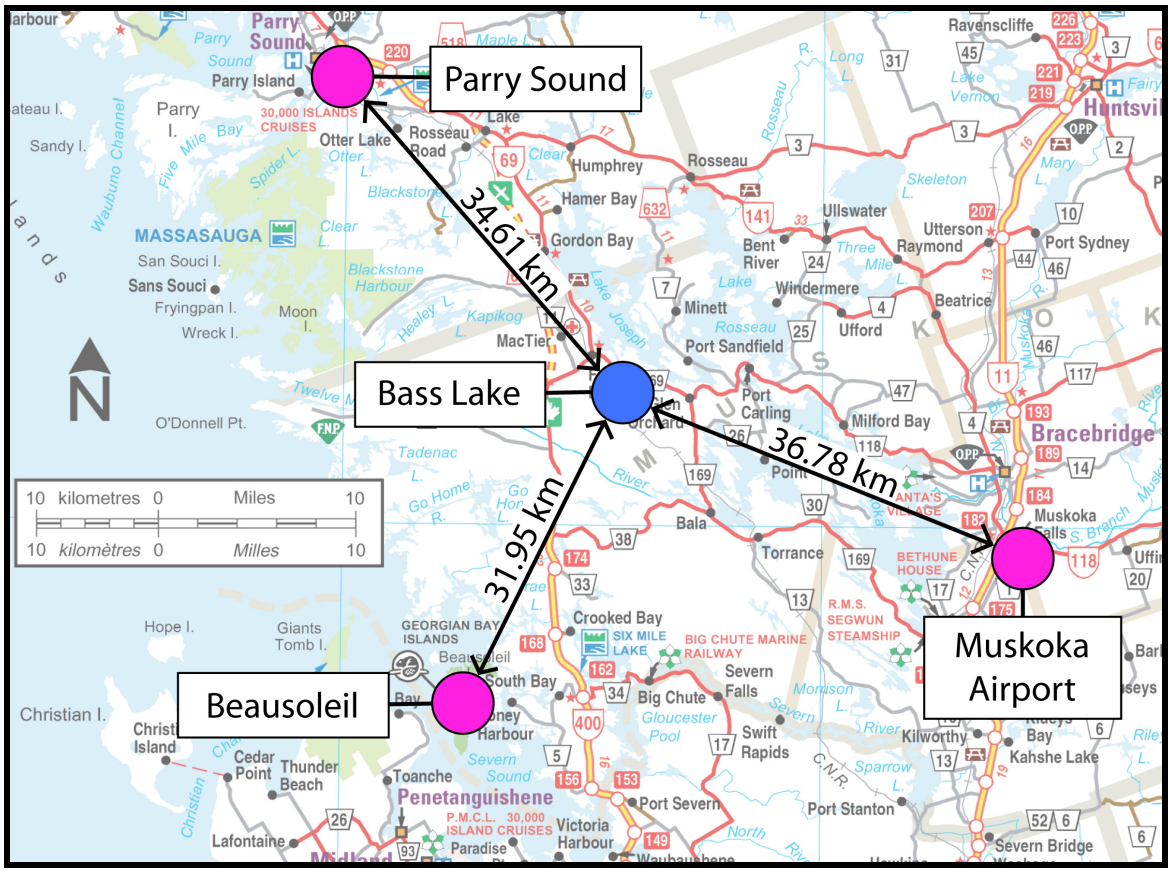

Figure 4.4.1 – Weather Station Locations (from MTO, 2005)

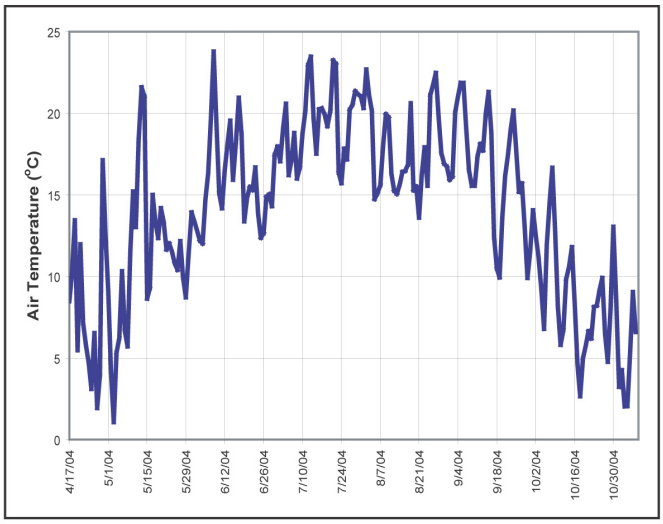

Figure 4.4.2 - Average Air Temperature

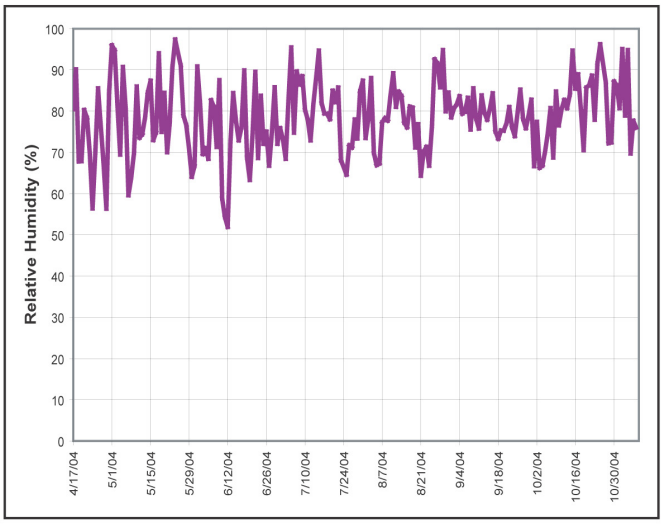

Figure 4.4.3 - Average Relative Humidity

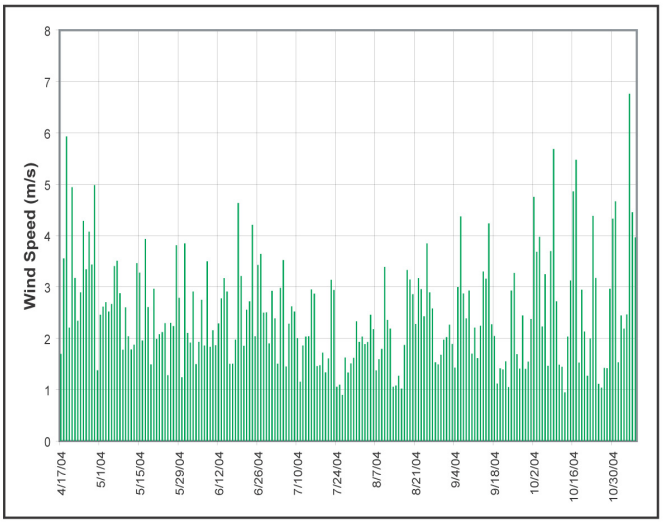

Figure 4.4.4 - Average Wind Speed

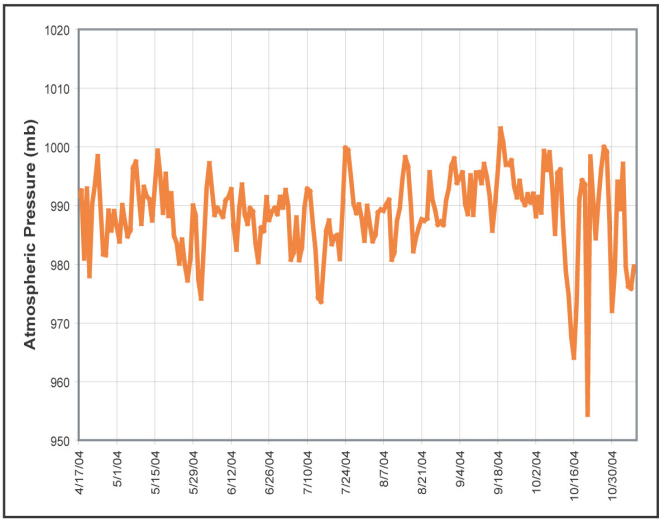

Figure 4.4.5 - Average Atmospheric Pressure

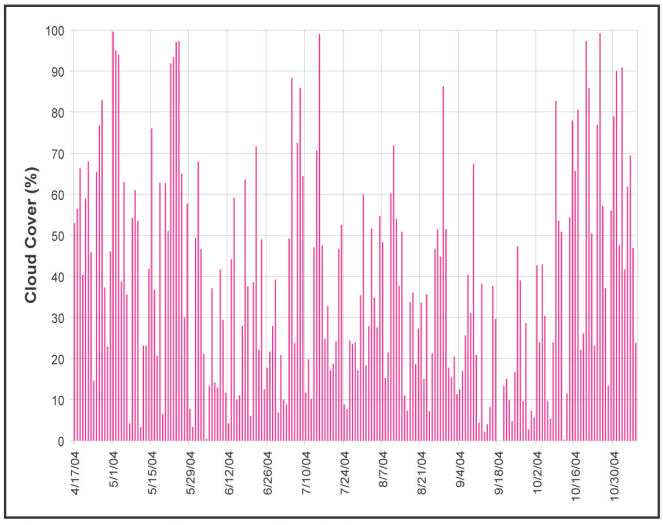

Figure 4.4.6 - Average Cloud Cover

4.5 LAND CLASS DATA

The land class (LC) designation is used in the elemental allocation of surface flow and evapotranspiration properties across the model domain. The LC data was acquired through the Minstry of Natural Resources Canada's GeoGratis website. The Ontario Land Cover map (1:250,000 scale) was incorporated with existing ArcView data and revealed four land cover categories for the model domain: surface water, dense deciduous forest, mixed forest, and sparse forest. Figure 4.5.1 presents the spatial distribution of the varying land covers across the model domain.

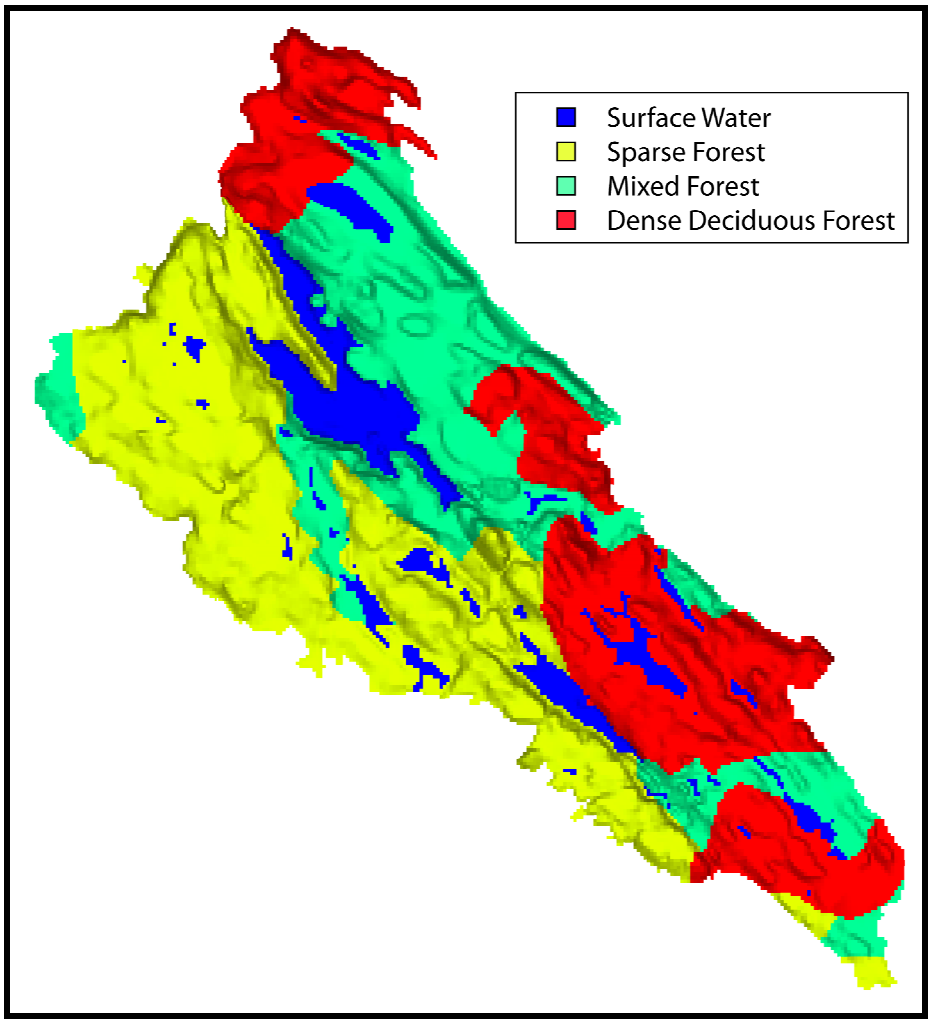

Figure 4.5.1 – Land Cover

The LC information was assigned to the elements across the watershed based on the position of each element centroid. As the scales of the OBM and LC map scales differed (1:10,000 to 1:250,000), the surface water elements were assigned from the known surface water bodies on the OBMs, while any inconsistencies with the outer water boundaries were also corrected in accordance with the OBMs.

Chapter 5

Model Setup and Parameter Definition

The quality of a numerical simulation model is limited by the quality and accuracy of the input data. For the Bass Lake model, every effort was made to ensure proper parameterization. The methods and sources used to define all model parameters are discussed herein.

5.1 Watershed Delineation

A watershed is defined as a closed region draining into a river or water body (Pearsall, 2005). The Bass Lake watershed was delineated using 1:10,000 scale Ontario Base Maps, connecting surface elevation highs around Bass Lake and all water bodies draining into it. The resulting catchment area was determined to be 6.24 km^2 and is shown on Figure 5.1.1.

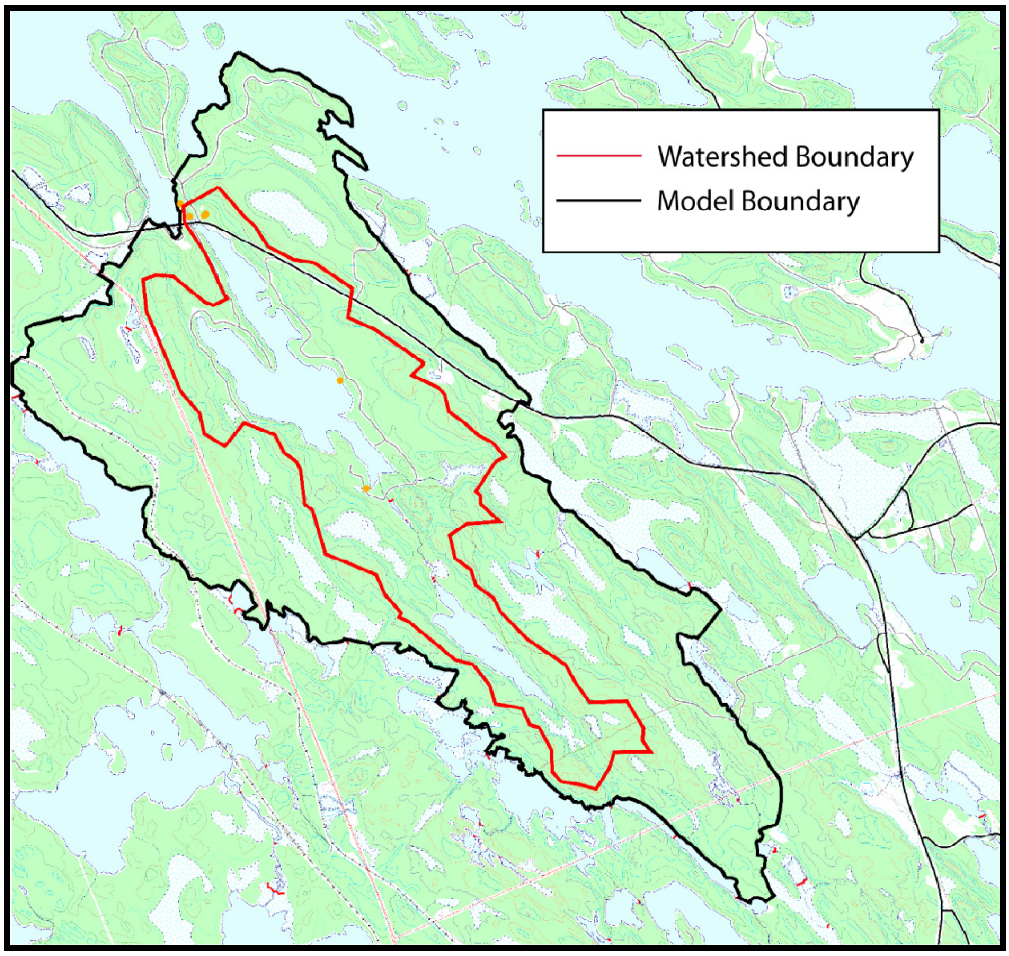

Figure 5.1.1 – Watershed and Model Boundaries

5.2 Model Boundary Definition

Conventional approaches to groundwater modelling use the outer watershed boundary as the maximum extent of the modelled domain. This model boundary definition assumes that the groundwater catchment boundaries directly coincide with the surface water catchment area. In the case of the Bass Lake study, the frequency of fractures and major geologic contacts did not support the conceptual construction that the surface water and groundwater catchments coincided. As such, the modelling domain was extended to account for these discontinuities. The model domain covers a surface area of 17.7 km^2 and is shown on Figure 5.1.1. The increased domain size allows for groundwater table highs to migrate as dictated by the transient flow conditions.

5.3 SURFACE GRID DEFINITION

Groundwater and surface water models are influenced by the surface element grid used to define the model domain. Proper grid sizing and areas of grid refinement can yield an accurate numerical simulation, while improper sizing and refinement can lead to increased computation times and even to invalid simulations. The definition of the Bass Lake model domain surface grid is described in detail in the following sections.

5.3.1 Finite Element Grid

An integrated modelling code, such as HydroGeosphere, that simultaneously solves groundwater, surface water, and evapotranspiration components, can require extensive computational resources. To minimize the computational burden, optimization of the model mesh is crucial. Triangular prism meshes allow for smaller element sizes that readily conform to complex and irregular defined boundaries (such as lakes, rivers and stream edges) and allow for larger elements within the interior of the domain. The development of HydroGeoSphere as a finite element integrated model offers the ability to use triangular prism finite element grids.

The triangular prism mesh was created using the Triangle (Shewchuck, 2004) two-dimensional mesh generator. The mesh was generated to meet Delaunay triangulation criteria. The element sizes were intensively refined at all water bodies within the Bass Lake catchment area and slightly refined for all remaining water bodies within the modelled domain. The resulting mesh surface mesh contains 15252 nodes, 29553 elements, and is shown on Figure 5.3.1.

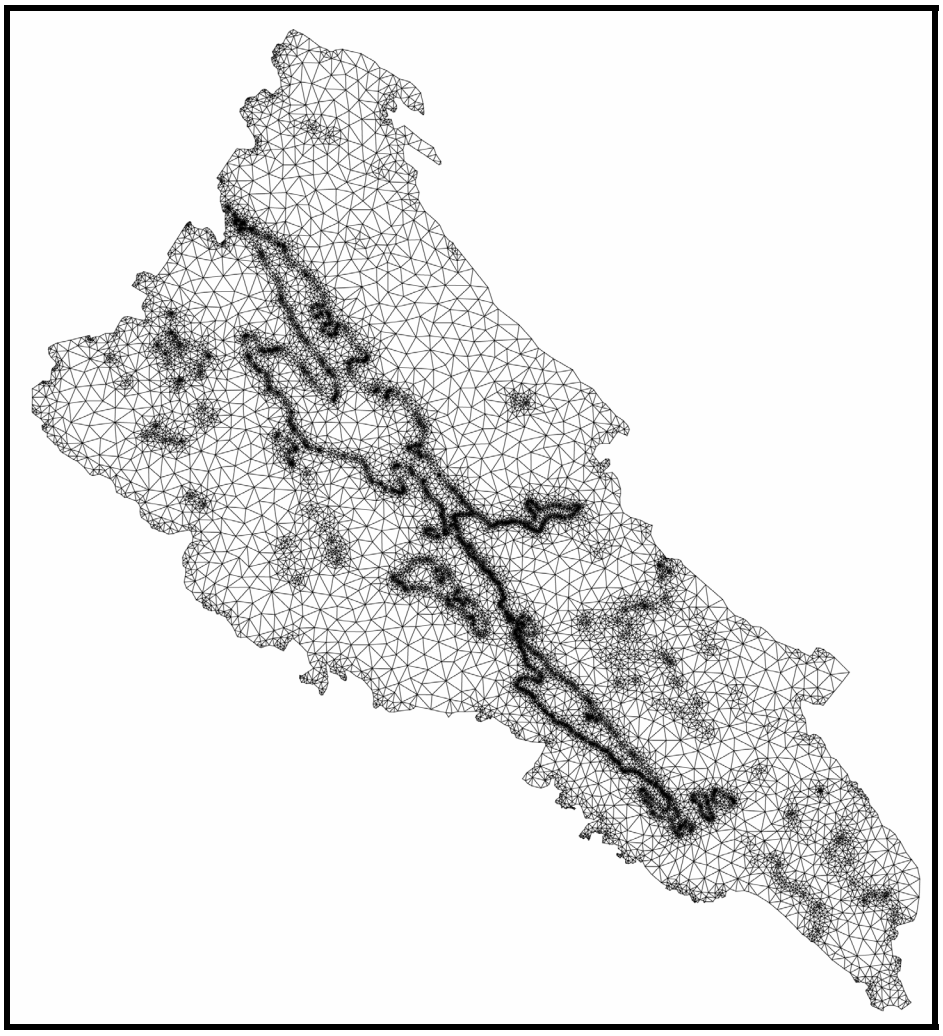

Figure 5.3.1 – Finite Element Grid

Numerous simulations were attempted using the finite element grid and its propagated subsurface layers. During these simulations, it became apparent that the finite element approach to solving the Bass Lake integrated system was too great of a computational burden for the resources available at this time. It was therefore determined that the present stage of HydroGeoSphere development can not accommodate the finite element approach for the Bass Lake model domain. Through personal communications with McLaren (2005b), a senior HydroGeoSphere developer, and through small-scale sub-watershed simulations, it became evident that a finite difference approach could offer simulation results given the computational resources available. The improved computational efficiency of the finite difference scheme can be attributed to the

decreased number of connection points used in solving the groundwater heads. A finite difference coefficient matrix is smaller and the repeated assembly of this matrix (for every timestep) will require less computational effort than would the same problem using using a finite element scheme.

5.3.2 Finite Difference Grid

The generation of a finite difference grid, using only quadrilateral elements, was completed using the Grid Builder two-dimensional mesh pre-processor (McLaren, 2005a). Maximum grid block sizes were set to 625 m^2 (25 m x 25 m). The north end of Bass Lake, corresponding to the watershed hydraulic control, was refined to ensure proper model mesh geometry. The grid blocks were refined to 6.25 m^2 (2.5 m x 2.5m), increasing at a rate of 1.2 times outside the area of interest to the maximum 25 meter by 25 meter grid block size. The completed two-dimensional quadrilateral element mesh contains 48693 nodes, 47761 elements and is shown on Figure 5.3.2.

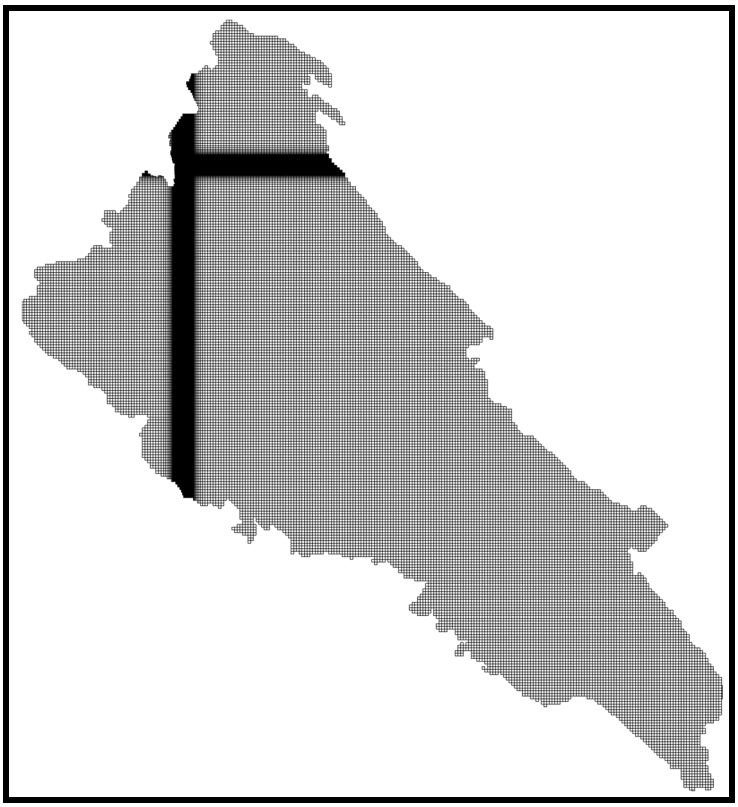

Figure 5.3.2 – Quadrilateral Finite Difference Grid

5.3.3 Digital Elevation Model Correction

Topographic contour lines from the digital Ontario Base Maps, as detailed in Chapter 4.2, were used to create an initial DEM. Results of visual field inspections and the Bass Lake bathymetric survey were added to the DEM to compliment the existing topographic data and to create realistic bathymetry for all water bodies within the watershed.

Following the addition of bathymetric features, a correction function was applied to the DEM. The original surface map created from the surface contours connected adjacent contour lines with straight lines as detailed on Figure 5.3.3.

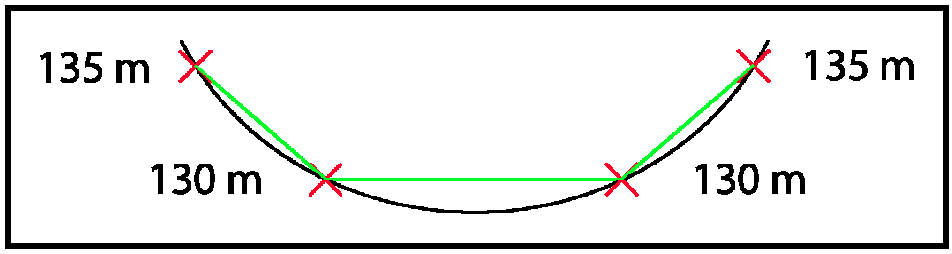

Figure 5.3.3 – TIN Generation Method

The hilltops and valleys bottoms were not accurately represented by the straight line interpolation. To correct these flat areas, the surface correction function examined the entire model domain and located these areas. The function then transformed the existing flat surface into a smoothed curve while conforming to the topographic contours. The function steps are shown on Figure 5.3.4.

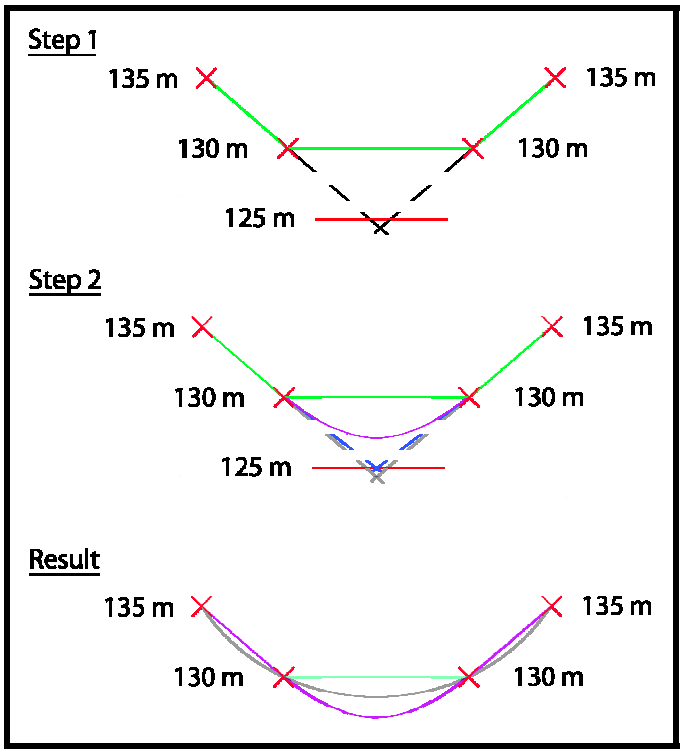

Figure 5.3.4 – DEM Correction Function Methodology

Step 1 of the function establishes whether a projection of the lines connecting topographic contours would violate existing surface contours. Figure 5.3.4 shows that a projection of the existing hill slope lines would cross another contour interval, thereby creating a topographic condition known not to exist.

Step 2 then computes the necessary corrections to the hill slope extensions by ensuring the extensions continue on an angle such that their intersection occurs prior to the next contour interval (dashed blue lines). If the result from Step 1 is shown to be consistent with the existing topographic contours, the angular correction is not performed. The function then fits a curved surface tangent to the origin of the hill slope extensions.

The resulting topographic surface (purple line) does not duplicate the existing topography (black line); however, the resulting surface is a more accurate and natural estimate, while avoiding the potential problems encountered with numerical simulations resulting from perfectly flat topographic surfaces. The resulting DEM is shown on Figure 5.3.5.

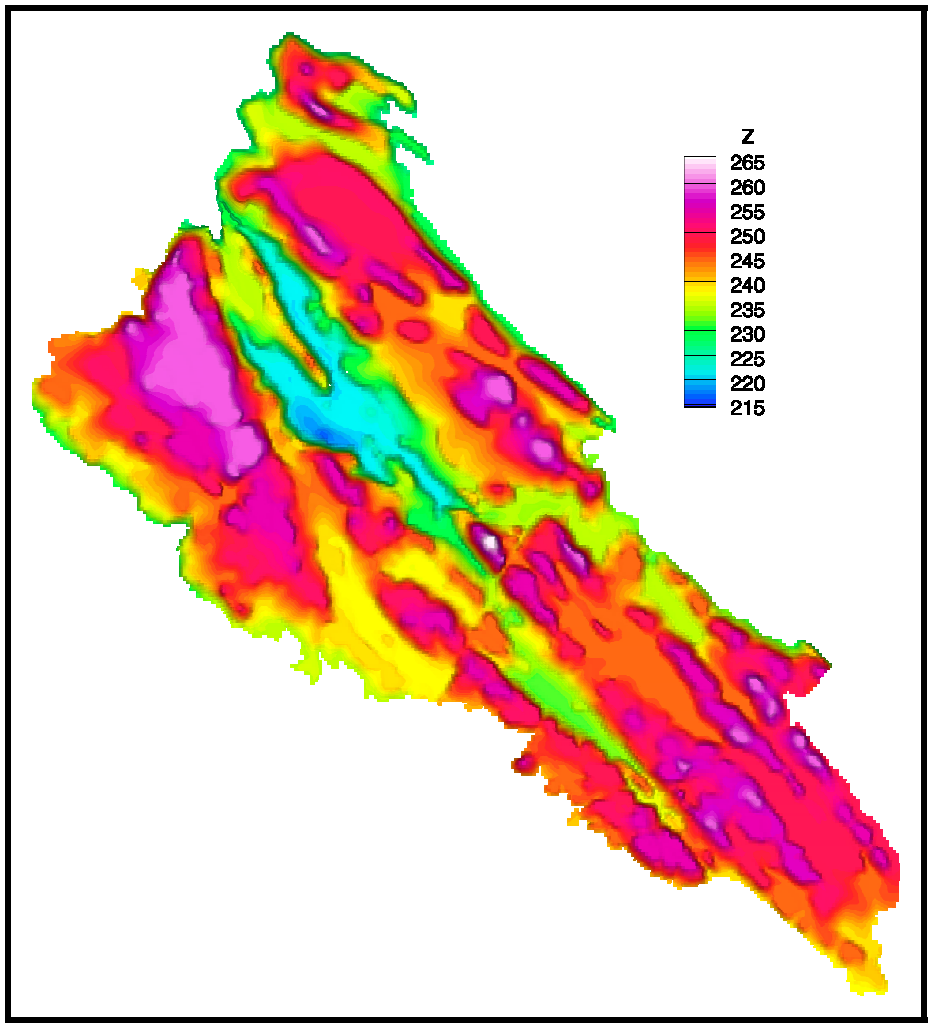

Figure 5.3.5 – Corrected Digital Elevation Model (masl)

The corrected DEM was used in assigning nodal surface elevations across the model domain.

5.4 Bass Lake Subsurface Definition

The Bass Lake model domain, located in the Canadian Shield, offers the opportunity to further study crystalline rock environments with integrated modelling simulations. The thin surface sediment layer combined with exposed fractured bedrock offers preferential pathways for the fluid flow between the groundwater and surface water flow regimes.

This section details the methods and sources used to define the Bass Lake model subsurface.

5.4.1 Surface Sediments

The location of the Bass Lake watershed offers a unique study site opportunity for the HydroGeoSphere model; however, the outcroppings of exposed fractured bedrock at surface offer extremely poor farming conditions. As a result, the Department of Agriculture and Agri-Food Canada, through the Canadian Soil Information System (CanSIS), has not completed any detailed soil surveys for much of the Muskoka district, including the entire Bass Lake watershed and model domain. As a result, the location and depth of surface soils have been assigned using randomized surface thickness distributions.

5.4.1.1 Location and depth of sediments

Water well records for the region were obtained from the Ministry of Natural Resources (2002). Twelve recorded water wells were found within the model domain (Figure 5.4.1).

In addition to the water well records, site investigations conducted between September 2002 and November 2004 yielded a maximum surface sediment depth of approximately 5.0 meters and a mean surface sediment depth of approximately 0.5 meters. The exposed bedrock at surface indicates a surface sediment depth of 0 meters, thereby corresponding to the minimum surface sediment depth. These values were used to ensure the proper range of surface depth distributions across the model domain.

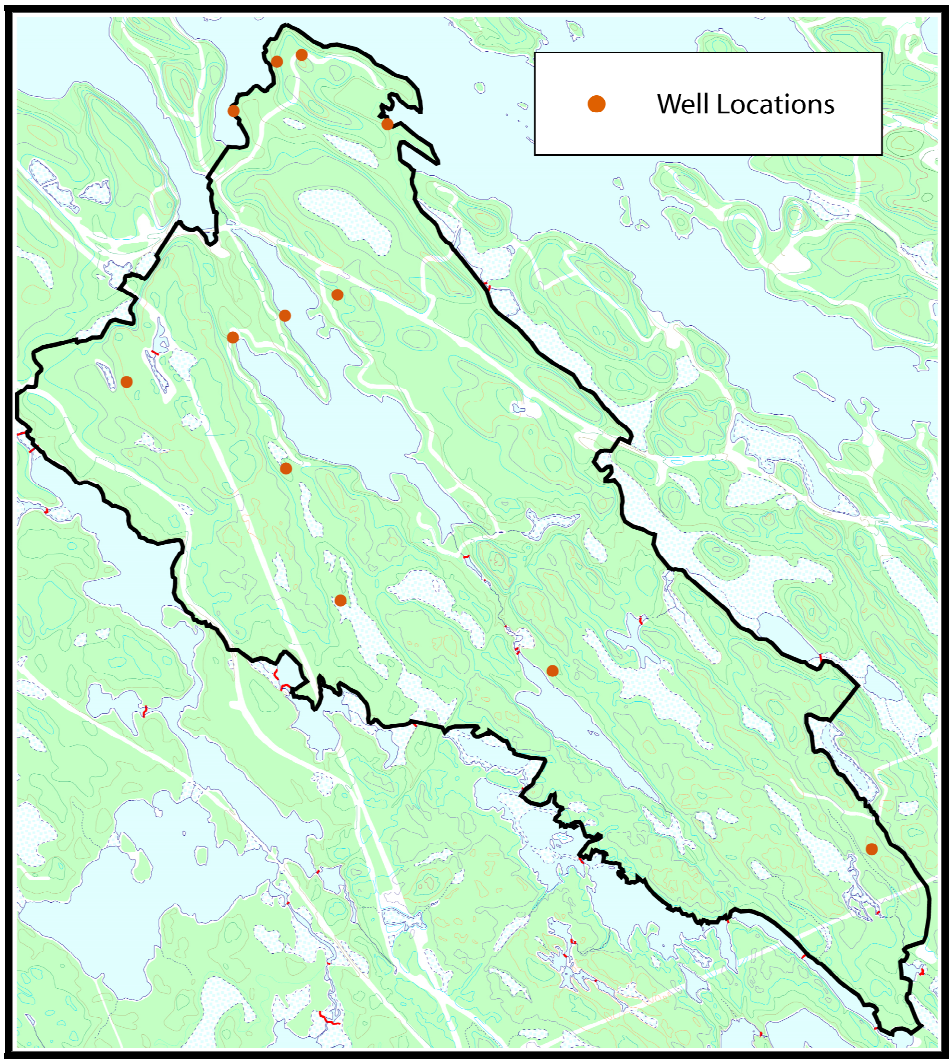

Figure 5.4.1 – Model Domain Water Well Locations

The locations of the surface sediments are variable across the watershed with the metamorphosed bedrock outcropping throughout. The location and extent of these outcrops are themselves quite variable, although they are influenced by topography and occur more frequently on peaks of hills rather than in valley bottoms. This topographic influence was the basis for the randomly generated surface thicknesses.

5.4.1.2 Surface Thickness Generation

A Fast-Fourrier Transform (FFT) random field generator (Robin et al., 1992) was used to generate random fields across the watershed. From observation during site visits and due

to the surface soil variability across the watershed, a correlation length of 30 meters was used. This correlation length implies that the surface sediments in one location are independent of those 30 or more meters away. The resulting random field distribution is shown on Figure 5.4.2.

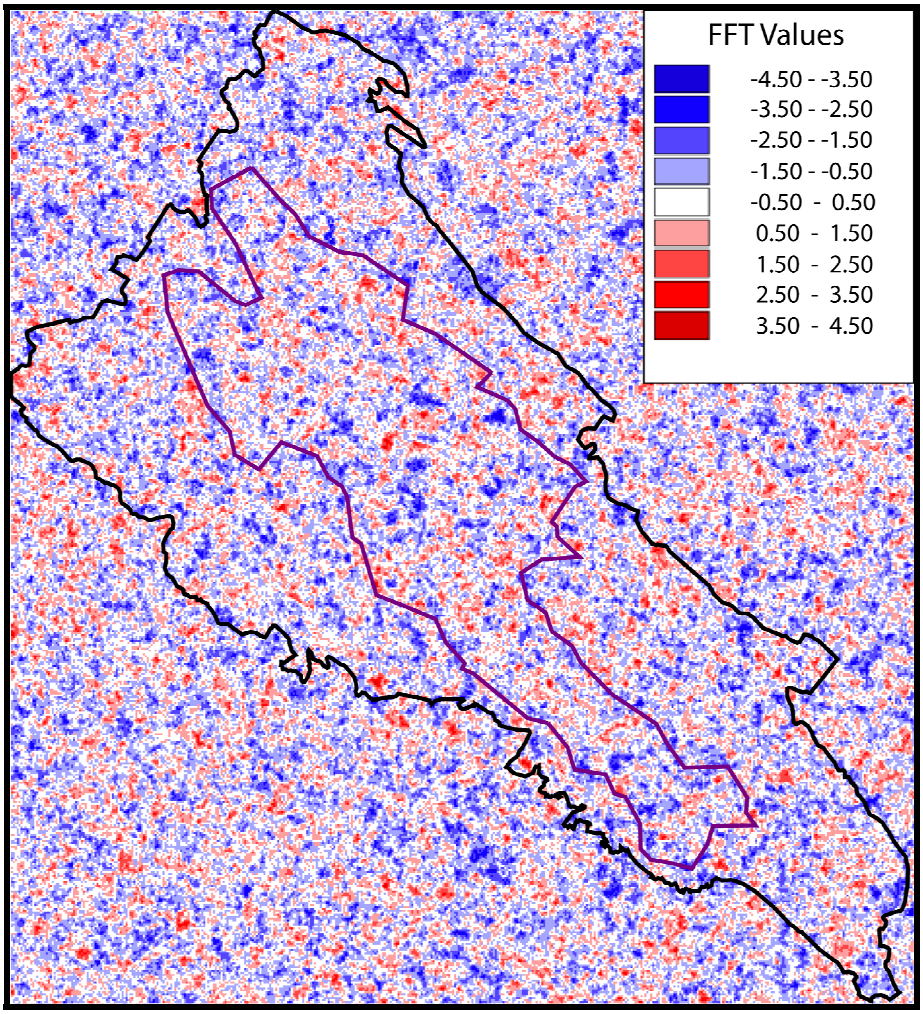

Figure 5.4.2 – Fast-Fourrier Random Field Distribution

To include the topographic influence, a surface smoothing function was created to determine convex and concave surface topography. The function calculates the average grid cell elevation for a 201 x 201 grid area, centered on the cell of interest. A smaller version of the grid setup is shown on Figure 5.4.3. The average cell value was then compared to the center cell value. A negative difference between the center cell and

average values corresponds with a concave condition (valley) while a positive difference corresponds with a convex condition (hill) (Figure 5.4.4).

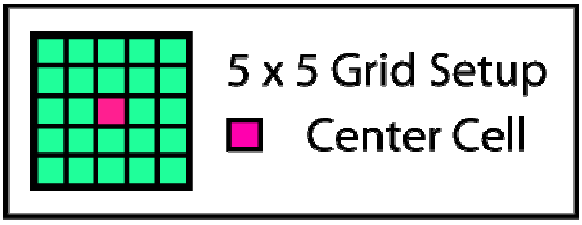

Figure 5.4.3 – Surface Smoothing Grid Setup

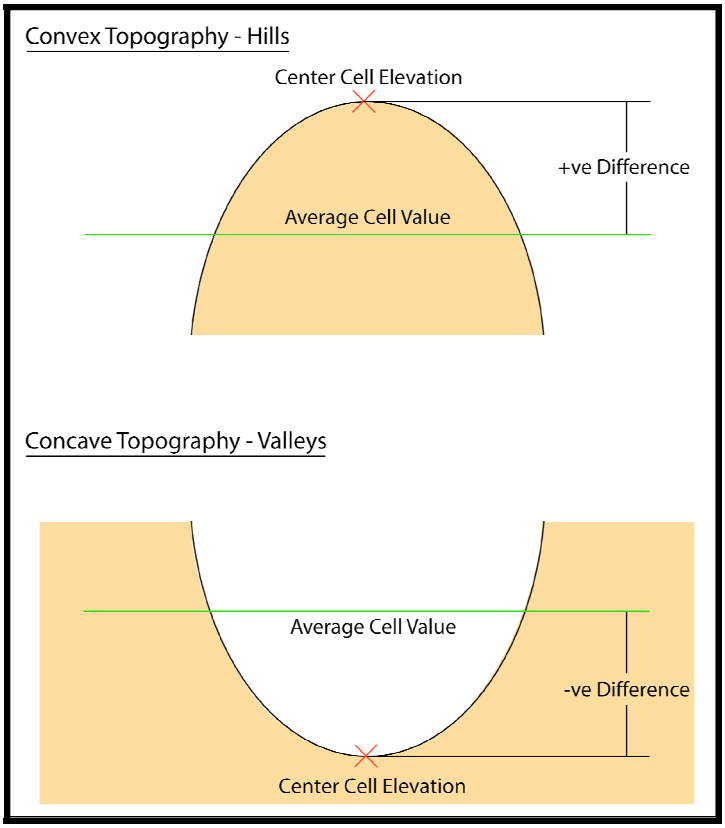

Figure 5.4.4 – Surface Smoothing

The smoothed surfaces were then normalized to yield maximum and minimum values of +1 and -1 respectively. Any values along the margins that could not be calculated were assigned a normalized value of 0. The resulting grid is shown on Figure 5.4.5.

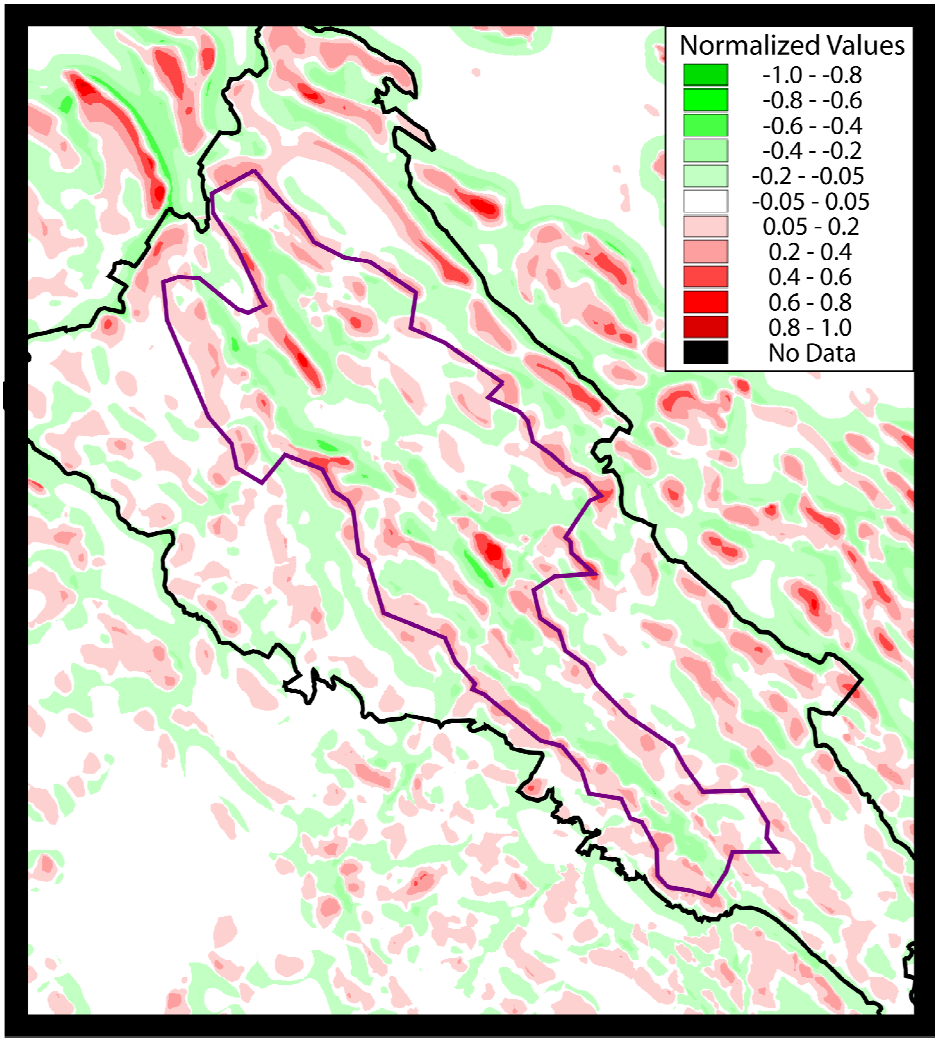

Figure 5.4.5 – Normalized Smoothed Surface

The FFT and normalized smoothed surface values were determined at each node location and combined to produce the surface sediment locations and depths. The FFT values were initially found to follow a normal distribution; however, they were transformed to follow a log-normal distribution to ensure non-negative surface depths. The surface depths, in meters, were computed using the following equation

$$Surface\ Thickness = (Norm + 1)\ x\ 10^{(a + (b\ x\ FFT))} \tag{5.1}$$

where *Norm* is the normalized smooth surface value, *FFT* is the generated Fast-Fourrier Transform random field value, and *a* & *b* are functions of the log-normal well record median and surface thickness standard deviations.

The resulting surface thickness has a maximum value of 4.81 meters, a minimum value of 0.00 meters, a median value of 0.39 meters, and an average value of 0.43 meters. The surface sediment distribution is shown on Figure 5.4.6.

Due to the random nature of the surface sediment distribution, there are potential locations across the watershed that have underestimated or overestimated sediment thicknesses. However, the random distribution of the surface sediments was calculated for a ground surface which itself is quite random. The final surface sediment distribution conforms to documented subsurface logs and offers a reasonable estimate of the overall surface sediment thicknesses given the minimal available data.

As determined through the soil sampling field program, the surface sediments were assigned properties consistent with silty sand. A summary of the properties is shown in Table 5.4.1.

Table 5.4.1 – Surface Sediment Properties

	Hydraulic Conductivity (m/s)	**Porosity (-)**	**Specific Storage (m^{-1})**
Silty Sand	2.0×10^{-5}	0.44	1.0×10^{-6}
Reference	*Schroeder et al., 1997*	*Schroeder et al., 1997*	*Schroeder et al., 1997*

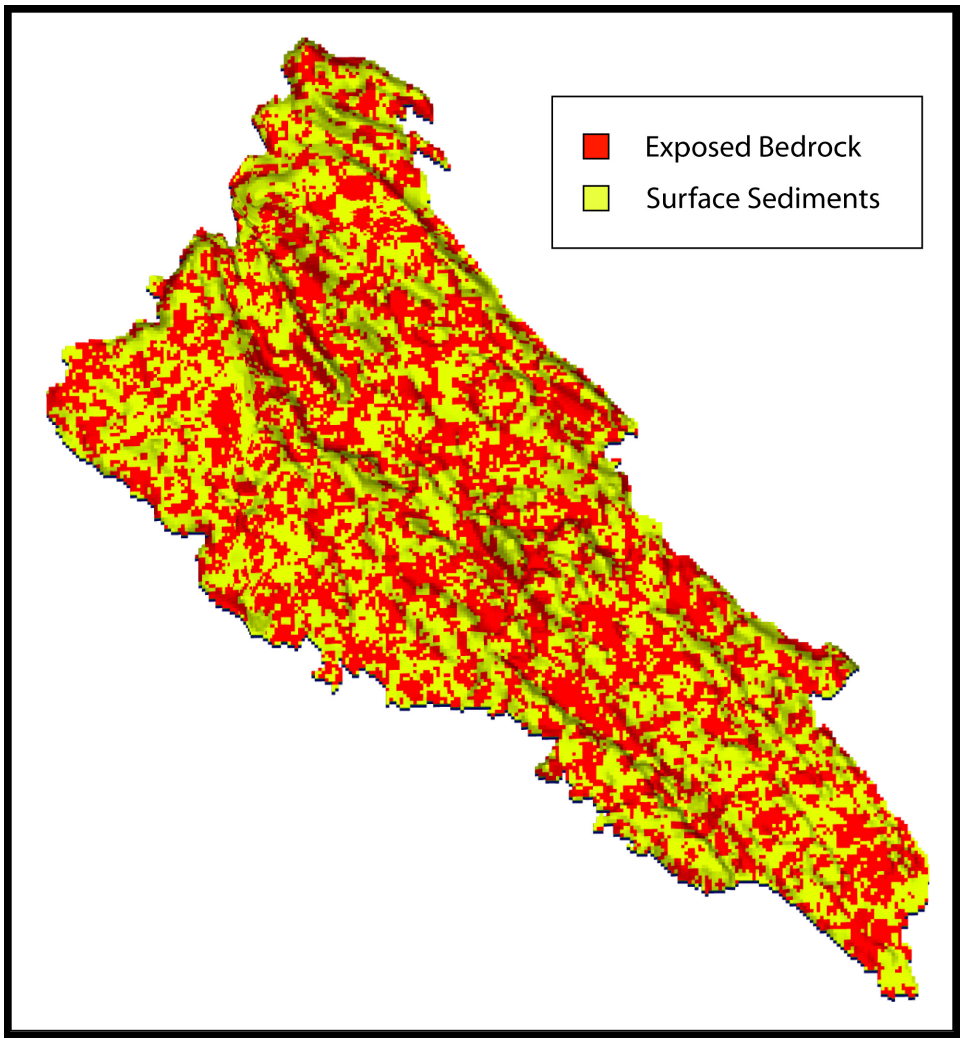

Figure 5.4.6 – Surface Sediment Distribution

5.4.2 Fractured Bedrock

As is consistent with many locations across the Canadian Shield, numerous vertical fractures exist across the model domain. The surface expression of these fractures can be seen in air photos and in the digital elevation model (Figure 5.3.5). Due to the computational burden and the uncertain simulation times for dual continuum integrated models, the domain subsurface is represented with equivalent porous mediums (EPMs). The EPMs are consistent with the Atomic Energy of Canada Limited (AECL) Lac du Bonnet, Manitoba subsurface characterization (AECL, 1994), as well as the Ontario Power Generation sub-regional groundwater modelling efforts (Sykes et al., 2003).

The subsurface consists of three layers of fractured bedrock: weathered bedrock, shallow bedrock, and deep bedrock. The weathered bedrock is directly below the surface sediments, and in some locations, is expressed as exposed bedrock. The bedrock within this layer is influenced by weathering and erosion processes. The main effect of these processes is increased hydraulic conductivities resulting from fracture propagation induced by numerous freeze-though cycles. The weathered bedrock extends from the bottom of the surface sediments to a depth of 4 meters below surface.

The shallow bedrock is assumed to be largely unaffected by weathering; however, its hydraulic conductivity is higher than that of the deep bedrock. This layer extends from 4 meters below surface to 14 meters below surface. The deep bedrock is the least hydraulically conductive layer and extends from 14 meters below surface to 26.5 meters below surface. The properties of all fractured bedrock layers are given in Table 5.4.2.

Table 5.4.2 – Fractured Bedrock Properties

	Hydraulic Conductivity (m/s)	**Porosity (-)**	**Specific Storage (m^{-1})**
Weathered Bedrock	5.0×10^{-6}	2.0×10^{-3}	2.2×10^{-7}
Shallow Bedrock	7.0×10^{-7}	2.0×10^{-3}	2.2×10^{-7}
Deep Bedrock	7.0×10^{-8}	2.0×10^{-3}	2.2×10^{-7}
Reference	*Sykes et al., 2003*	*Sykes et al., 2003*	*Sykes et al., 2003*

To facilitate the variably saturated flow conditions, the discretization of the subsurface begins with small element thicknesses near surface, with element thicknesses increasing with depth. Figure 5.4.7 illustrates the subsurface discretization.

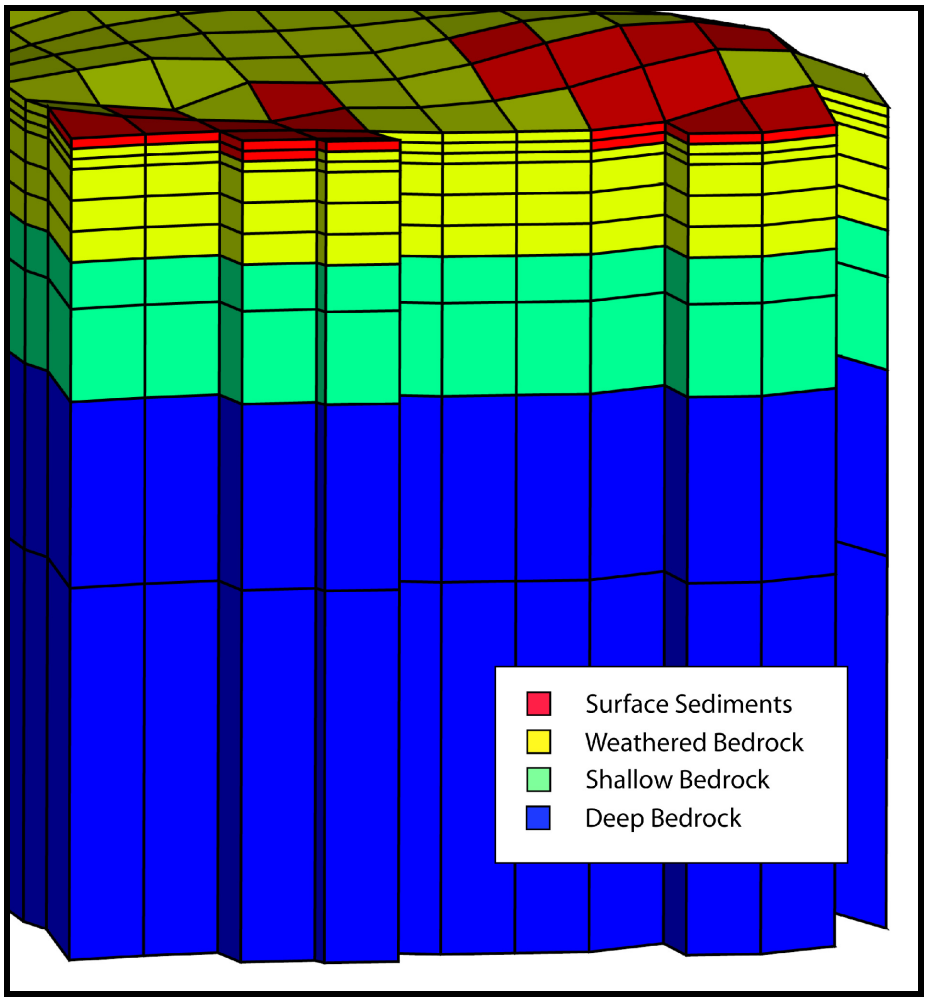

Figure 5.4.7 – Subsurface Grid Discretization (10x Vertical Exaggeration)

5.5 Overland Flow Properties

The surface flow within a model domain is controlled by the existing natural features. Many of the existing surface features are difficult to quantify at the grid scale (eg. broken tree branches impeding surface flow and increasing local rill overland storage values); however, these features are taken into consideration in determining the average overland flow parameters.

The overland flow parameters were assigned based on the land cover designation discussed in Chapter 4.5. The parameters were assigned to the surface faces of the elements based on the location of the element centroid. Due to similar surface covers

within the three forest land covers, all non-water body elements were assigned equal overland flow parameters. The friction factors, rill storage heights, and bottom leakance factors for the land covers are shown in Table 5.5.1.

Table 5.5.1 – Overland Flow Parameters

	Friction Factor ($s/m^{(1/3)}$)	**Rill Storage Height (m)**	**Bottom Leakance Factor (s^{-1})**
Mixed Forest	0.03 to 0.06 (x- & y-)	0.0001	0.02
Sparse Forest	0.03 to 0.06 (x- & y-)	0.0001	0.02
Dense Deciduous Forest	0.03 to 0.06 (x- & y-)	0.0001	0.02
Water Body	0.025 to 0.05 (x- & y-)	-	0.05
Reference	(Bras, 1990)	-	-

5.6 BOUNDARY CONDITIONS

The Bass Lake model domain requires the designation of three differing boundary conditions: Dirichlet, Neumann, and evapotranspiration or Type III boundary conditions.

The Dirichlet, or Type I, boundary conditions are defined as constant head boundary conditions. Their application was limited as the surface and subsurface water bodies are connected with the linkage term discussed in Chapter 3.3. However, as the model domain was extended to the next adjacent water body or topographic low, Dirichlet boundary conditions were required along the outer model boundary to allow the exit of excess groundwater from the model. Any outer boundary node located adjacent to a water body was assigned a constant head boundary condition equal to the surface elevation of that node.

The Neumann, or Type II, boundary conditions are defined as fluid flux boundary conditions. In traditional groundwater models, Neumann boundary conditions are

applied to represent groundwater recharge, pumping or injection wells, or any withdrawal or addition of a mass of fluid to a model. The HydroGeoSphere integrated model calculates the groundwater recharge based on the surface water-groundwater linkage term and therefore requires no explicit definition of fluid flux between the surface and subsurface flow regimes. In addition, no major pumping or injection wells are located within the model domain; therefore, no Type 2 boundary conditions are applied.

As the driving force for groundwater and surface water flow and transport, accurate precipitation input values are required for the model. The daily precipitation values collected during the precipitation sampling program are used to describe the transient precipitation conditions applied to the surface layer of the domain.

5.6.1 Historical Data Inverse Distance Weighting Approach

A great deal of the climate data required to accurately estimate the evaporation within the Bass Lake model domain was not feasible to include as part of the field data collection programs. To obtain the required data, as discussed in Chapter 4.4, climate data were obtained from Environment Canada for the three weather stations closest to Bass Lake. However, weather data can be largely variable across an area the size of the modelling domain, let alone across distances like those between the weather stations and Bass Lake. To account for this variability, given the data sets available, an inverse squared distance weighting approach was used to determine the values within the watershed.

Inverse squared distance weighting is an interpolation method that weights the data such that the influence of a data point declines with its distance from the point of interest. The inverse squared distance weighting equation specific to Bass Lake is

$$Weighted\ Data\ Value = \frac{\left[\frac{Data_{ParrySound}}{Dist_{ParrySound}^{2}} + \frac{Data_{Beausoleil}}{Dist_{Beausoleil}^{2}} + \frac{Data_{MuskokaAirport}}{Dist_{MuskokaAirport}^{2}}\right]}{\left[\frac{1}{Dist_{ParrySound}^{2} + Dist_{Beausoleil}^{2} + Dist_{MuskokaAirport}^{2}}\right]} \quad (5.24)$$

where $Data_x$ is the data value at location x and $Dist_y$ is the distance from location y to Bass Lake.

5.6.2 Calculated Maximum (Reference) Evaporation

The watershed maximum evaporation values are required input parameters for the evapotranspiration component of HydroGeoSphere. The weighted historical climate data was used for the Bass Lake maximum evaporation calculations. A simplifying assumption of water temperature was required to augment the data set.

The Muskoka Lakes Association (MLA) collects bi-weekly water samples from several locations in major lakes across the Muskoka district (MLA, 2004). Dissolved oxygen content, phosphate levels, and water temperature are several of the parameters of interest. With no available water temperature data from within the model domain, the values from Lake Joseph were examined. The collected water temperatures from Lake Joseph were not transferable to Bass Lake, as the average water depths and water temperature profiles differ greatly between the lakes.

To account for the lack of available data, several potential time-lagged water temperature approximations were formulated and examined. These functions approximated the water temperatures using weighted daily average air temperature functions that weighted recent daily air temperature values more heavily than previous days. Without collected water temperatures within Bass Lake, calibration of the resulting water temperature estimates was not possible. As a result, the surface water temperature was set to equal the daily air temperature. The water temperature used in the evaporation calculations is that of a thin

film at the water surface. Given this information and with minimal available data, the use of this assumption is reasonable. The daily maximum evaporation values calculated for the duration of the study period and are presented on Figure 5.6.2.

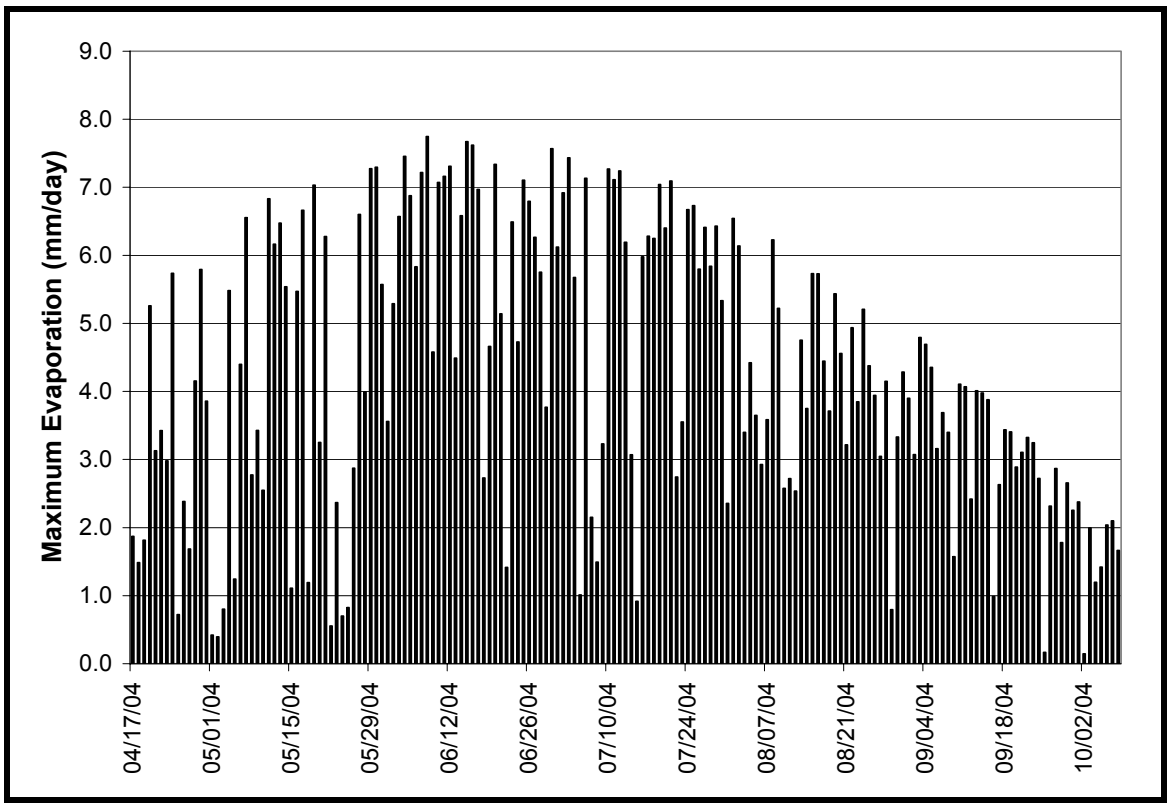

Figure 5.6.1 – Calculated Daily Maximum Evaporation

5.6.3 Additional Evapotranspiration Properties

The evapotranspiration properties determined for the model domain are fairly similar in nature, differing only slightly between land cover classes. Surface element faces defined as surface water were assigned a leaf area index (LAI) of 0 and a root depth of 0 m. The mixed forest, sparse forest, and dense deciduous forest land covers were assigned the values as shown in Table 5.6.1.

Table 5.6.1 – Evapotranspiration LAI and Root Depth Values

	Max. Leaf Area Index	Root Depth
Mixed Forest	3.290	2.0 m
Sparse Forest	2.580	2.0 m
Dense Deciduous Forest	3.605	2.0 m
Reference	*Scurlock et al., 2001*	*Canadell et al., 1996*

The evapotranspiration input requires soil properties for the surficial layers of soil from which the vegetation roots draw their water. Only two subsurface layers were affected (due to the maximum root depth of 2m), the silty sand and weathered bedrock, and their averaged evapotranspiration properties are shown in Table 5.6.2.

Table 5.6.2 – Evapotranspiration Soil Properties

	Wilting Point (vol/vol)	Field Capacity (vol/vol)
All Land Cover Classes	0.06	0.15
Reference	*Schroeder et al., 1997*	*Schroeder et al., 1997*

5.7 MODEL MONITORING

To monitor the model results and ensure proper model functioning during and upon completion of modelling runs, a hydrograph and an observation well were included within the model.

5.7.1 Hydrograph

The hydrograph was included to observe the surface water discharge from the northern end of the Bass Lake watershed. The hydrograph output was used to ensure steady state simulations had reached steady state, as transient flow models with constant input conditions were used to complete the steady state modelling. The hydrograph was

located downstream of the natural rock weir, along the discharge channel for the watershed. The nodes across which flow is monitored are shown on Figure 5.7.1.

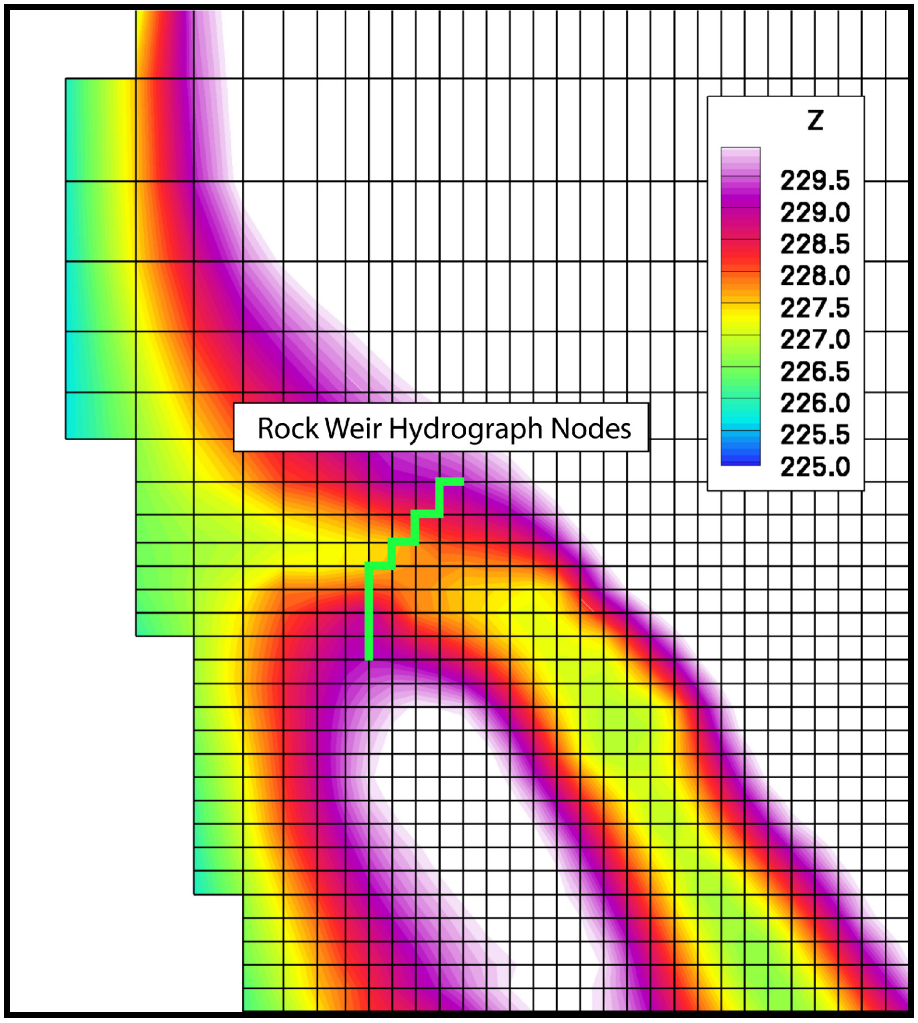

Figure 5.7.1 – Hydrograph Node Location

5.7.2 Observation Well

To compare and calibrate the modelled lake level response to precipitation events with the collected Bass Lake water elevation data, an observation well was created to record total head within the well for every model time step. The observation well was located within Bass Lake, away from the lake boundaries to minimize the influence of exfiltration on the recorded total heads.

5.8 MODEL ITERATION AND SOLVER CONVERGENCE CRITERIA

The HydroGeoSphere model iteration and solver convergence criteria are values that can be used to modify model accuracy and efficiency. These values were altered to maximize model run times while ensuring appropriate model water balance. The maximum allowable water balance error was 1% of inflow.

Chapter 6

Results and Discussion

The Bass Lake model domain simulations were completed with 2 different precipitation conditions; one using actual precipitation and reference evapotranspiration (ET) values (ET component activated), with the second using a precipitation input value equal to the actual precipitation minus reference ET (no ET component). These two conditions are subsequently referred to as the unsaturated and saturated simulation henceforth. The following chapter presents and discusses the responses of the coupled groundwater and surface water flow systems.

6.1 GROUNDWATER FLOW RESULTS

The groundwater results for the Bass Lake domain simulations are presented herein; however, they are presented without the benefit of accompanying observed groundwater system response data. As a result, the simulated groundwater responses will be compared to expected groundwater trends for the model domain.

6.1.1 Groundwater Heads and Flow Directions

The Bass Lake model domain groundwater heads are presented on Figure 6.1.1. The figure presents a general trend of decreasing overall head toward the Bass Lake watershed rock weir outlet to Lake Joseph. Decreased groundwater head occurs in regions of decreased topographic elevation and is consistent with the expected groundwater flow patterns. The local groundwater highs also mimic the previously delineated watershed divide boundaries.

A groundwater flow vector field for the north end of Bass Lake is presented on Figure 6.1.2. This figure shows the flow directions and relative magnitude with appropriately scaled flow vectors. This figure reinforces the conclusions drawn from Figure 6.1.1 in showing the flow directions trend, as expected, from topographic highs to topographic lows. A maximum groundwater flux rate of 1.885×10^{-5} m/s was observed. The observed flux rate is consistent with the hydraulic conductivities used in the model subsurface characterization.

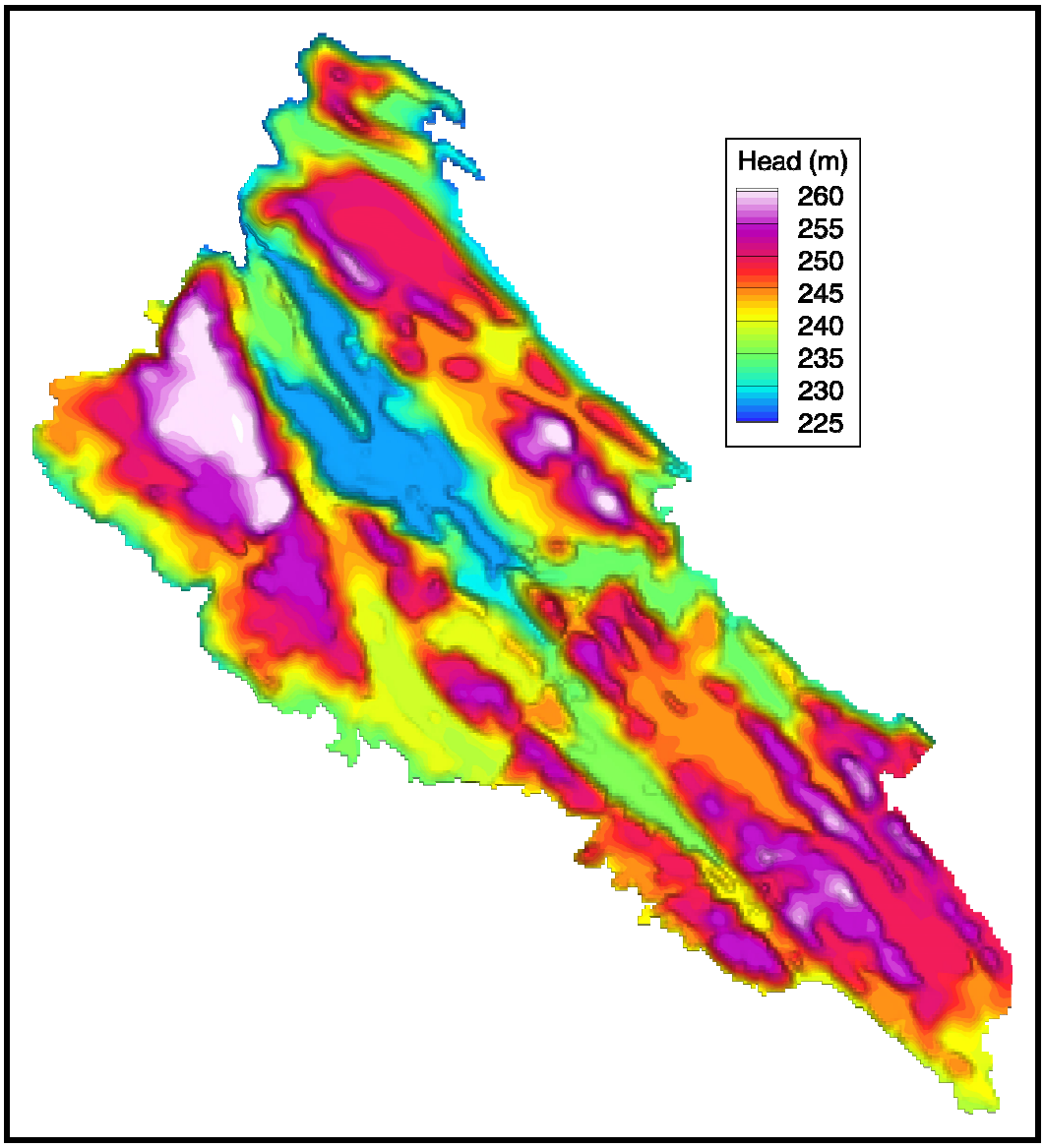

Figure 6.1.1 – Groundwater Heads (Unsaturated, t = 10 d, low overland n)

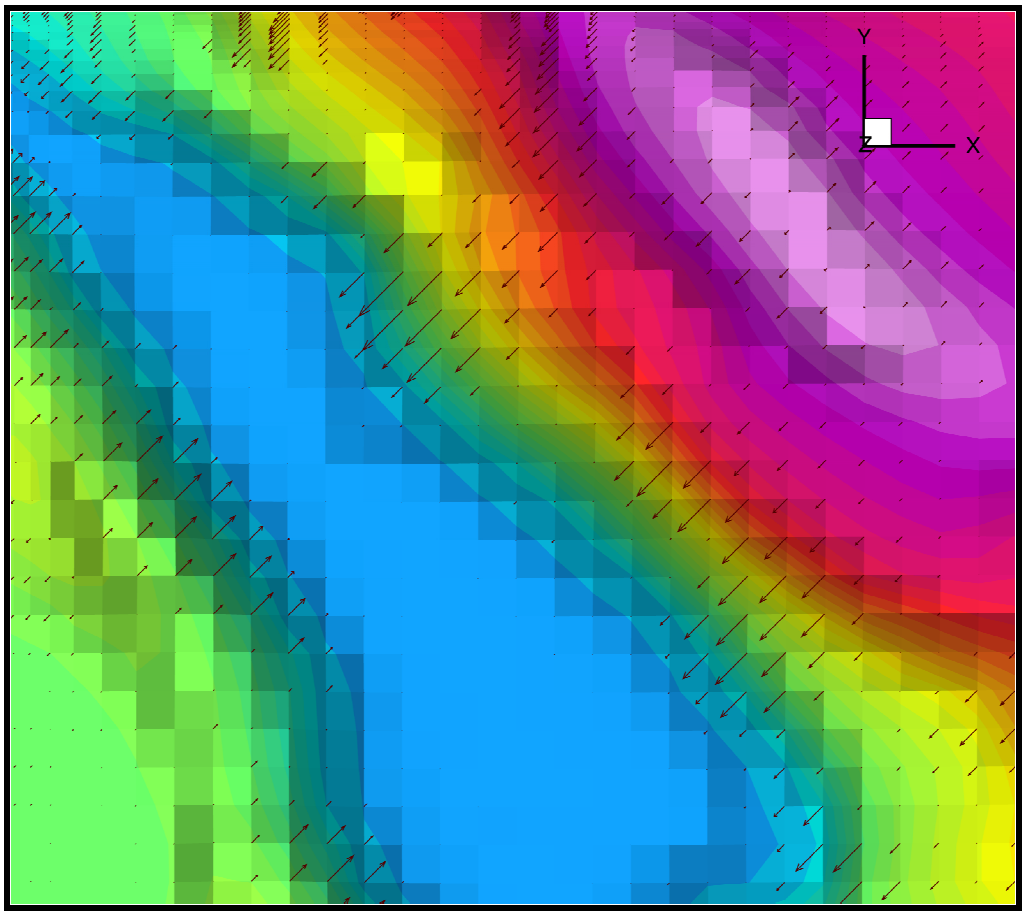

Figure 6.1.2 –Groundwater Flow Vector Field (Unsaturated, t = 10 d, low overland n)

6.1.2 Subsurface Saturation Levels

The subsurface saturation levels at ground surface are shown on Figure 6.1.3. The figure shows decreased saturation levels within the forested land cover areas across the domain. These decreased values appear as expected and show that the evapotranspiration component is depleting the subsurface saturation levels through plant transpiration. Fully saturated regions are illustrated in dark blue and represent locations of surface water ponding. Observed and modelled locations of fully saturated conditions (i.e. surface water bodies) correspond very closely, providing further validity to the modelled results.

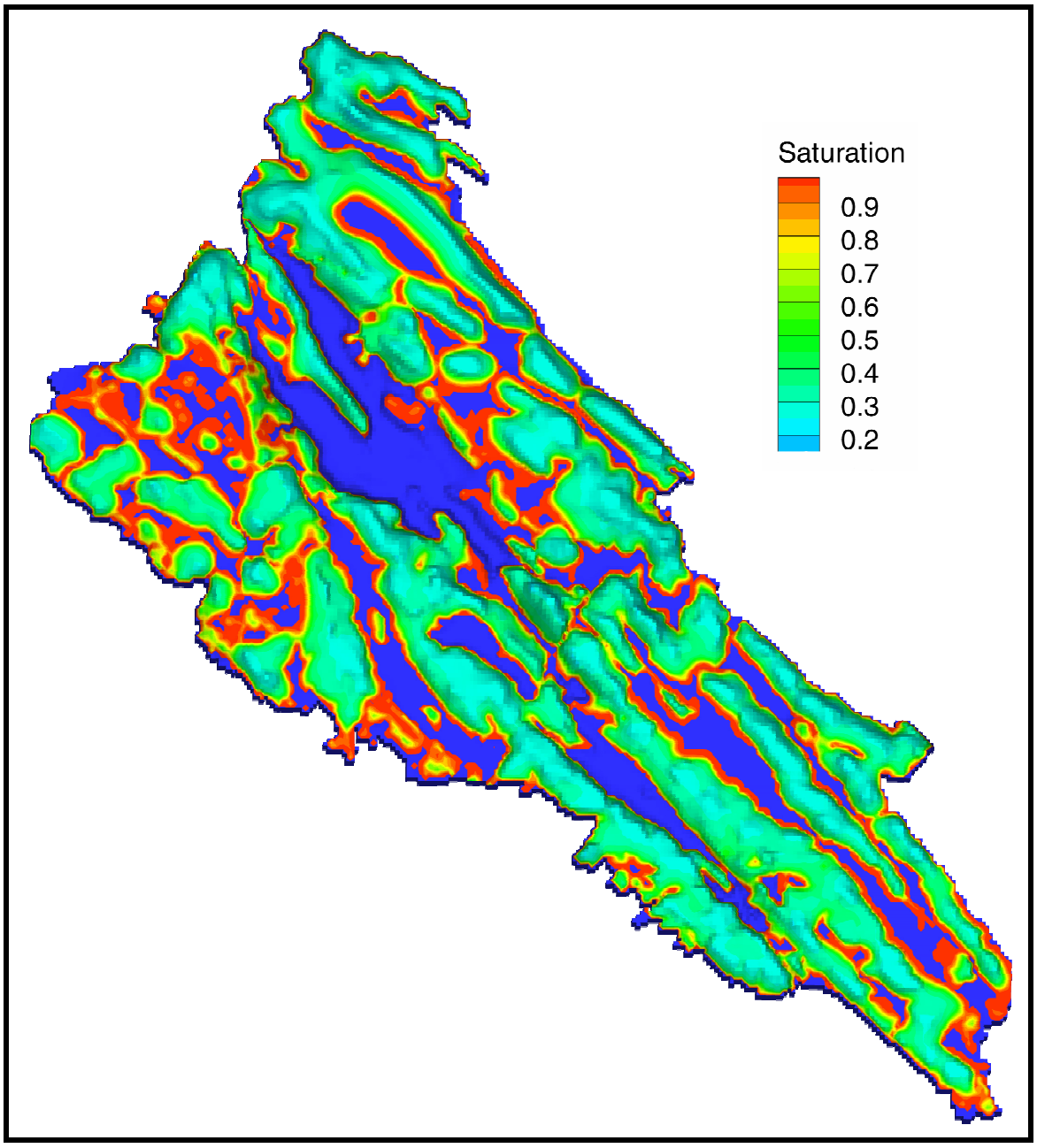

Figure 6.1.3 – Subsurface Water Saturation (Unsaturated, Steady State, low overland n)

6.2 SURFACE WATER FLOW RESULTS

The surface water results for the Bass Lake domain simulations were compared to observed Bass Lake water elevation response data. Results from unsaturated and saturated flow simulations are presented.

6.2.1 Surface Water Depth and Flow Directions

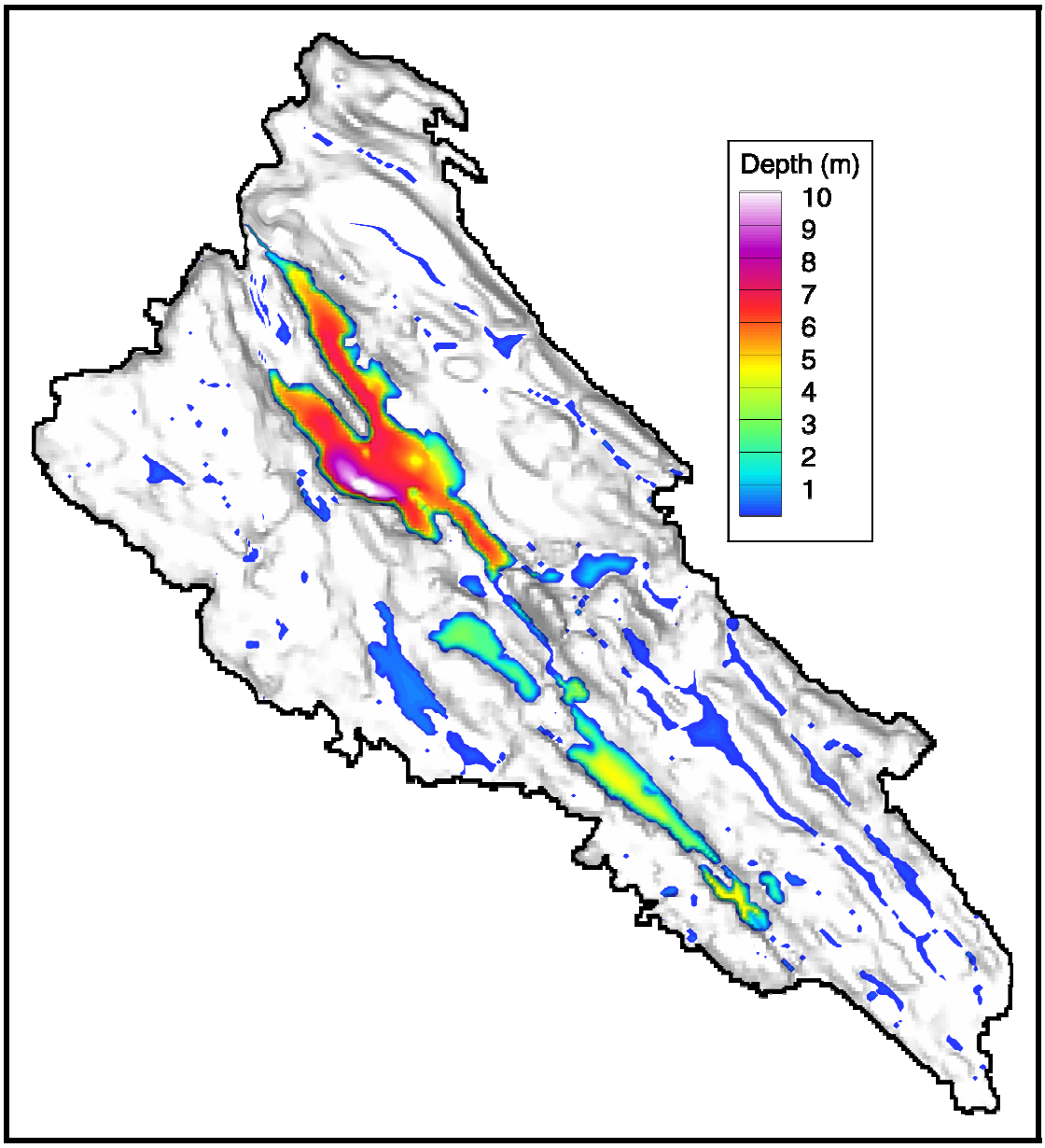

Figure 6.2.1 – Surface Water Depths (Unsaturated, t = 10 d, low overland n)

The surface water depths are presented in Figure 6.2.1. Only surface water depths greater than 0.001 m have been shown to illustrate areas of surface water accumulation. These surface water depths are consistent with the bathymetric survey results. Across the modelling domain, the locations of surface water accumulation are consistent with the air photos, digital Ontario Base Maps, and field observations.

A surface water flow vector field for the north end of Bass Lake is presented on Figure 6.2.2. This figure shows the flow directions and relative magnitude with appropriately scaled flow vectors. Maximum surface flow velocities of 1.4 m/s were simulated. The surface water flows within the watershed boundaries are moving towards Bass Lake; conversely, surface water flows outside of the watershed are flowing away from Bass Lake towards the model domain boundary. Water flow within Bass Lake is moving towards the north end and the watershed outflow to Lake Joseph.

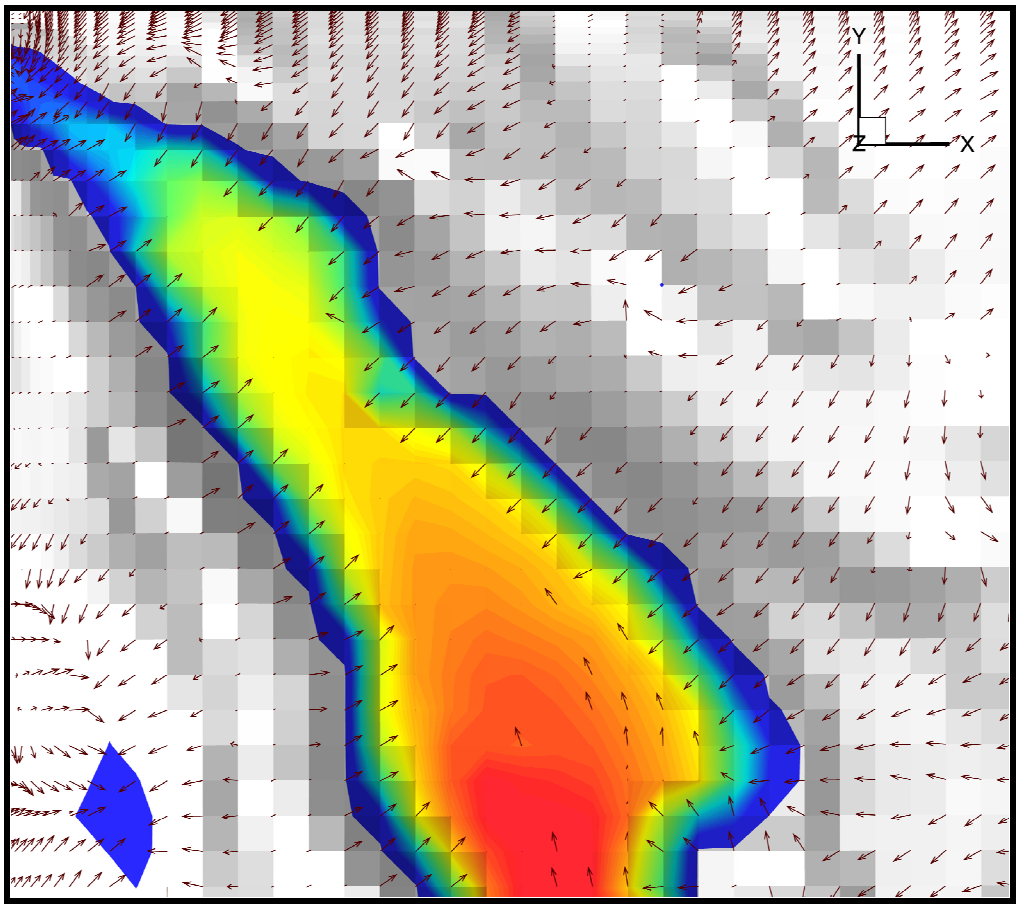

Figure 6.2.2 – Surface Water Flow Vector Field (Unsaturated, t = 10 d, low overland n)

6.2.2 Bass Lake Water Elevation Comparisons

The simulated and observed Bass Lake water elevations for the unsaturated and saturated flow simulations are presented below.

6.2.2.1 Saturated Flow Simulations

The saturated flow simulations were performed to compare simulation times and overall model performance. A 52-day simulation was performed to capture the Bass Lake response to a large precipitation event. These simulations accounted for the ET component by subtracting the ET from precipitation input (to a minimum of 0). The results of two simulations are presented in Figure 6.2.3: the first using a high overland Manning's n (0.06) while the second uses a low overland Manning's n (0.03).

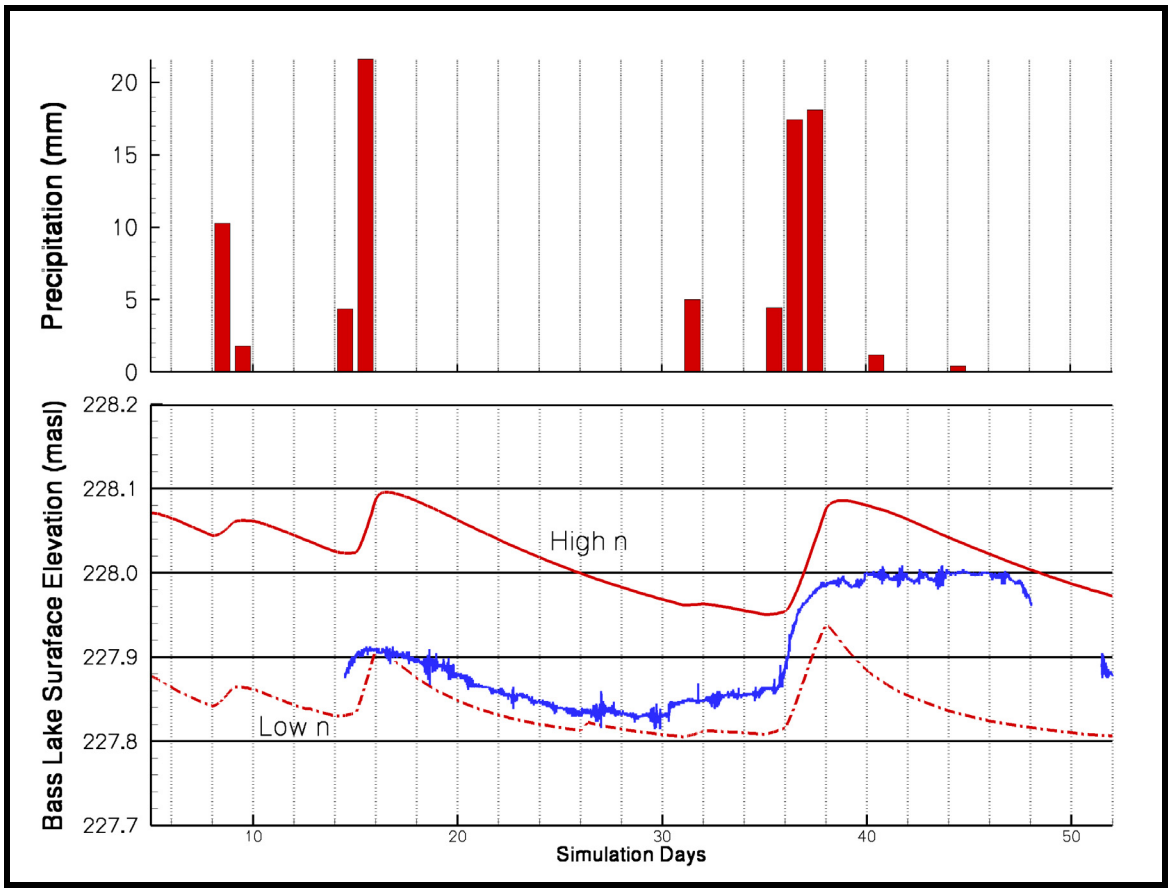

Figure 6.2.3 – Saturated Flow – Bass Lake Water Elevation Response

The simulated responses to precipitation events show similar water level increases throughout the 52-day simulation period. A time-lagged response of the simulated lake levels can be explained as a product of using daily averaged input values and as a product of using precipitation minus ET for precipitation input conditions. The overall lake level response is similar to the observed lake levels until day 38. Following the major storm event (day 36-38), lake level recession is noticeably faster than that observed. The difference in the simulated and observed lake levels could also be a function of the ever changing physical landscape of the model. Beaver dams have been observed at varying times and locations (at Bass Lake inlets and outlet) throughout the data collection season. Future studies could examine the possibility of accounting for the beaver dams; however, with minimal recorded beaver dam records, their influence on the Bass Lake watershed cannot be quantified.

A comparison of the low n and high n simulations shows that the low n model offers a more realistic overall Bass Lake water level. Examination of the major storm events at days 16 and 38 shows that the high n model water level decreases more gradually than does the low n model. This is expected from the increased surface friction that acts to decrease the speed with which the surface water flows within and out of the model.

6.2.2.2 Unsaturated Flow Conditions

The unsaturated flow simulations were performed, similarly to the saturated flow simulations, to compare simulation times and overall model performance. An 85-day simulation was performed to capture the Bass Lake response to seasonally varying flow. These simulations include the evapotranspiration component. The results of two simulations are presented on Figure 6.2.4: the first using a high overland n while the second uses a low overland n.

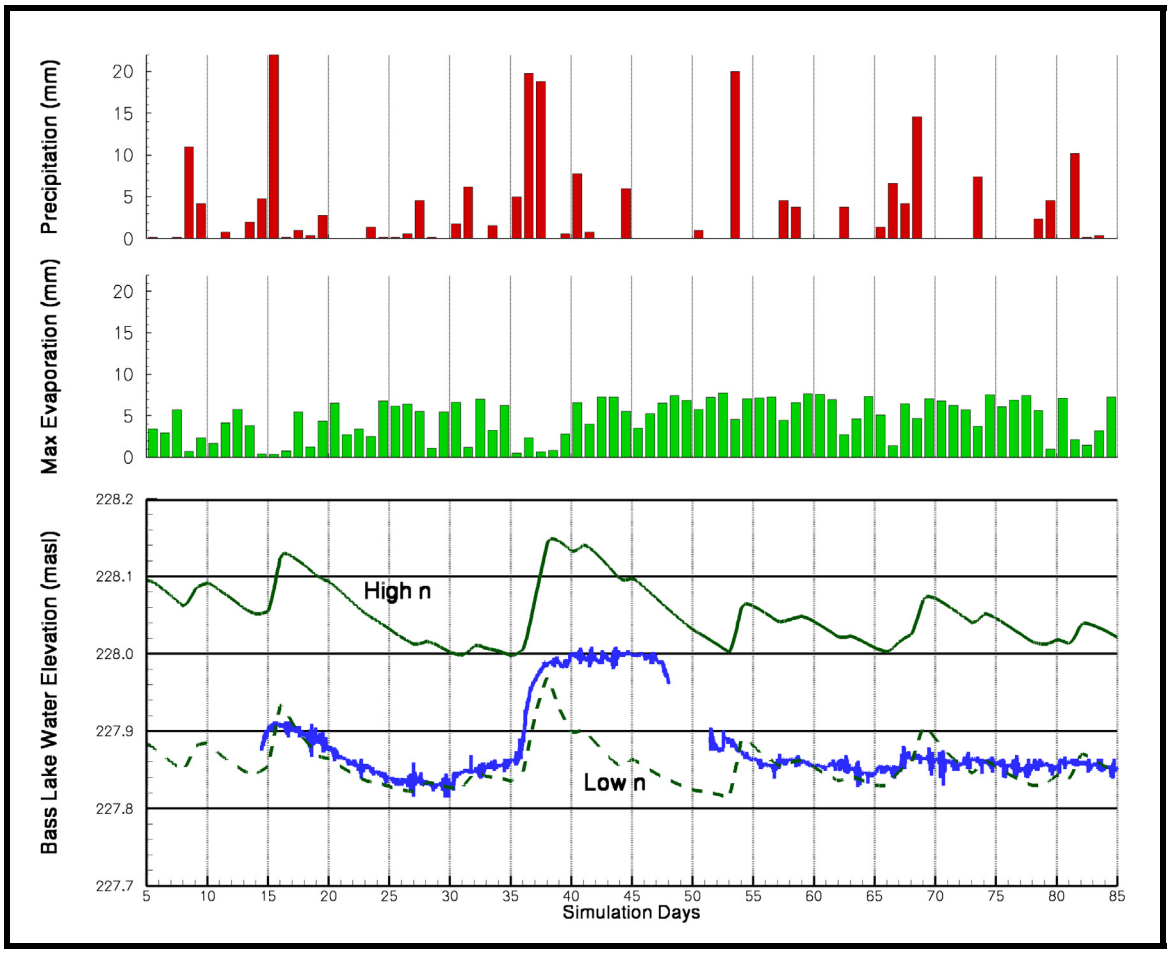

Figure 6.2.4 – Unsaturated Flow – Bass Lake Water Elevation Response

The simulated responses to precipitation events show similar water levels throughout the 85-day simulation period. Only a slight time-lagged response of the simulated lake level is observed and can be explained as a product of using average daily input values for the model or that overland flow had minimal influence in the context of soil storage or unsaturated conditions. The overall lake level response is similar to the observed lake levels until day 38. Following the major storm event (day 35-38), lake level recession is noticeably faster than that observed; however, the both unsaturated models show improved lake level recession limbs.

Similarly to the saturated flow simulations, a comparison of the low n and high n simulations shows that the low n model offers a more realistic overall Bass Lake water

level. Again, examination of the major storm events at days 16 and 38 shows that the high n model water level decreases more gradually than does the low n model.

6.2.2.3 Flow Condition Comparison

A comparison of all flow simulation models over 85 days is compared on Figure 6.2.5. This comparison shows that the unsaturated flow simulations both offer a more realistic response to the precipitation events occurring between day 30 and 36. It is apparent that the saturated flow simulations underestimate the Bass Lake water level throughout the duration of the simulations. Finally, it is apparent that the low overland n unsaturated flow model offers the most realistic Bass Lake water level simulation; however, all models overestimate the speed with which the water levels decrease following the major storm event starting on day 35.

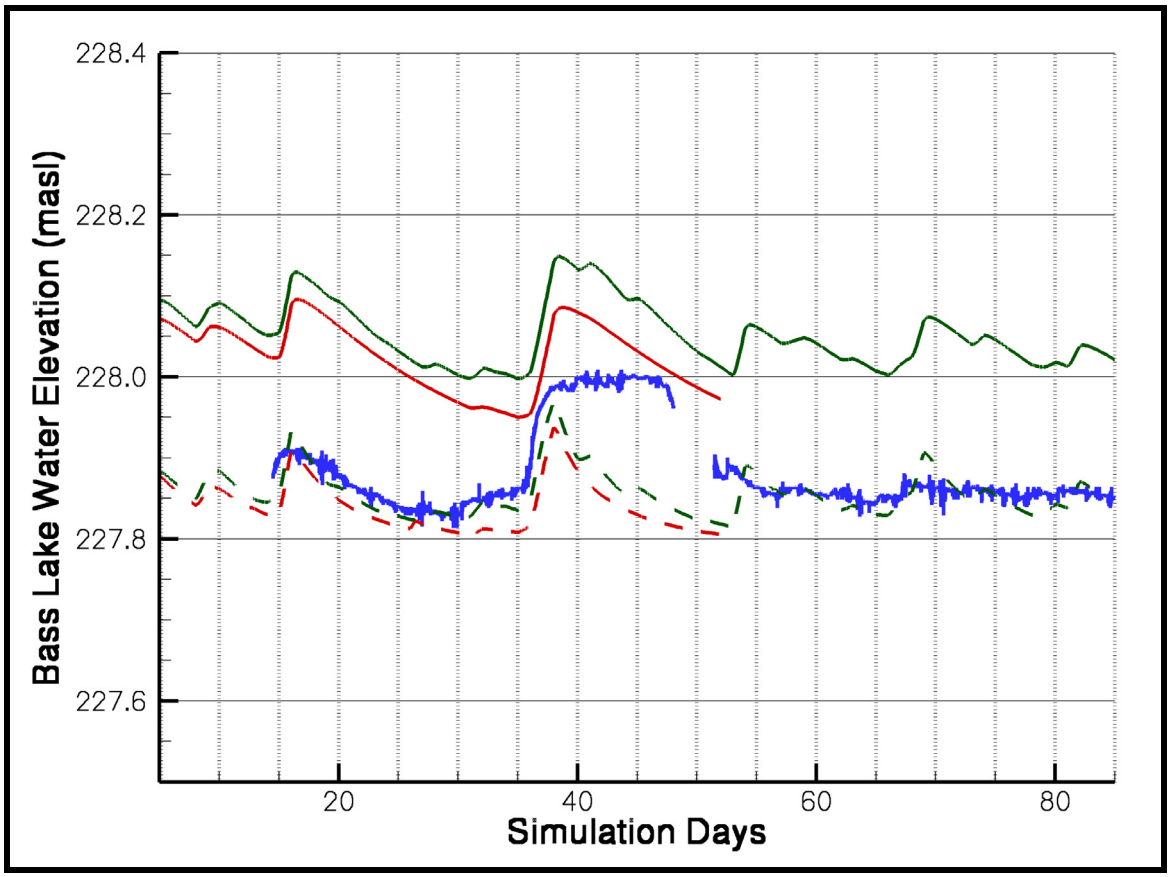

Figure 6.2.5 – Flow Comparison – Bass Lake Water Elevation Response

6.3 COUPLED FLOW RESULTS

The simulated flow between surface water and groundwater domains is expressed as an exchange flux and presented on Figure 6.3.1. A positive exchange flux travels into the surface water domain (exfiltration), while a negative exchange flux travels into the groundwater domain (infiltration). The maximum exfiltration occurs at the edges of surface water boundaries while maximum infiltration occurs at areas of relative topographic highs. These results are comparable to the expected physically based trends.

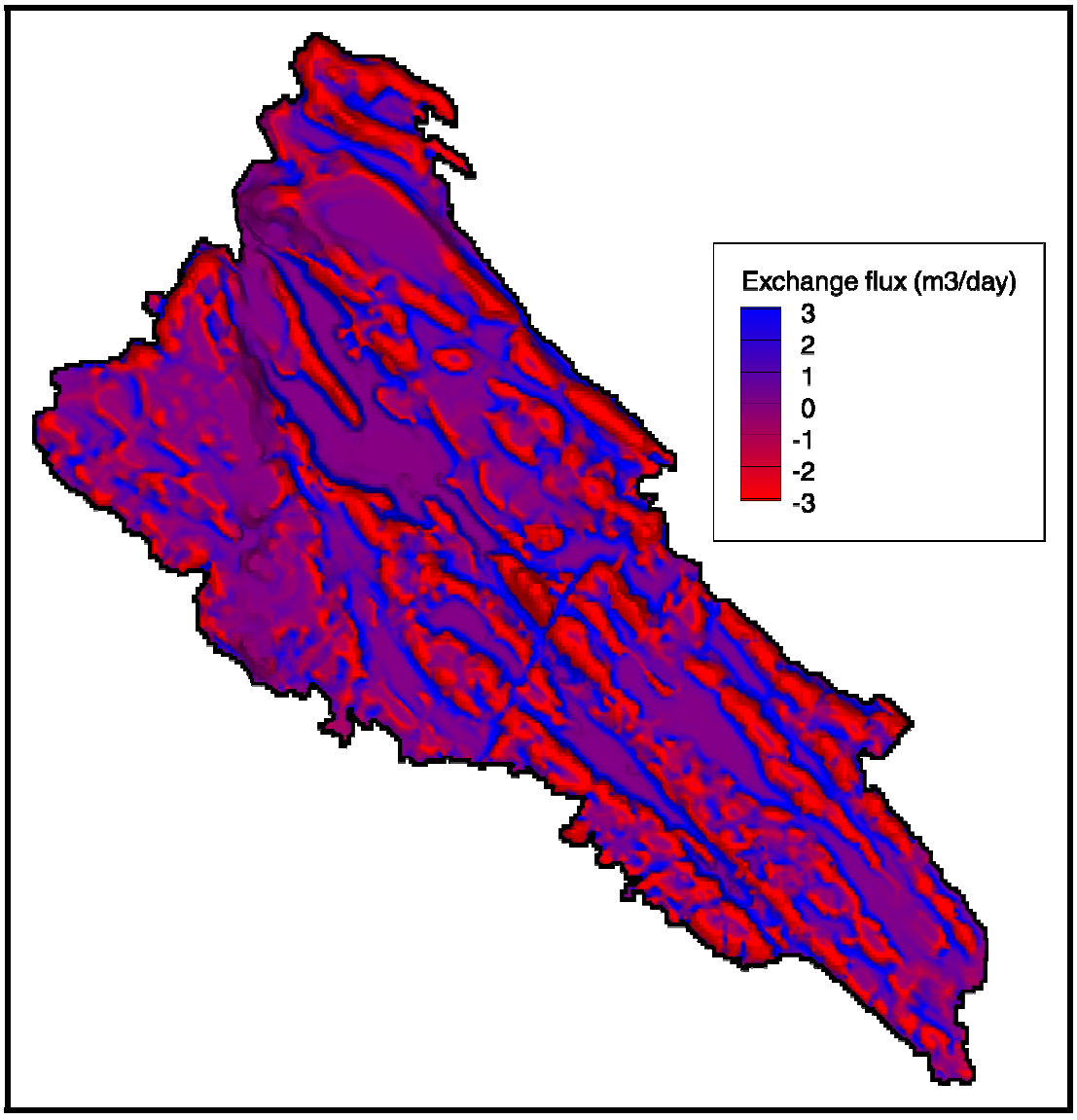

Figure 6.3.1 – Exchange Flux Between Subsurface and Surface Flow Domains

6.4 SIMULATION RUN TIMES

The model simulation times are presented in Table 6.4.1.

Table 6.4.1 – Simulation Run Times

Model Conditions	Sim. Run Time (Actual Days)	Sim. Length (Sim. Days)	Sim Day/Actual Day
Unsaturated, high overland n	10.3	175	17.0
Saturated, high overland n	2.6	52	19.8
Unsaturated, low overland n	7.8	85	6.7
Saturated, low overland n	3.7	52	14.2

Two general trends can be seen from the results. Firstly, simulation runs with high overland friction values run noticeably faster than those with low overland friction values. Higher overland friction values act to dampen the head fluctuations between timesteps. As a result, fewer solver iterations (on average) were required for the high overland friction simulation runs, thereby decreasing the run times.

Secondly, it can be seen that the unsaturated runs ran slower than the saturated runs. The saturated model runs did not include the evapotranspiration components and therefore required fewer calculations for each timestep, resulting in decreased model run times.

6.5 HYDROGEOSPHERE MODELLING CHALLENGES

The Bass Lake domain numerical simulations proved to be complex in nature and difficult to complete. Challenges throughout the project caused many setbacks, many extra hours of work, and many difficult times. As unwanted as these setbacks were, they are a reality when testing a research modelling code and can offer valuable feedback for model developers throughout the model development stage.

The challenges encountered during the design included, but were not limited to the following:

- Finding a robust Finite Element mesh generator and creating the required executable files for grid generation
- Model grid alteration from triangular Finite Element to rectangular Finite Difference
- Issues with the ET solver matrix assembly loops which caused simulation times to be five to six times slower than required
- File Access Termination Bug which stopped numerous model runs well into their simulation periods
- Critical Depth Boundary Condition setup alteration to increase pre-processor speed

Chapter 7

Conclusions

Conceptual integrated surface water-groundwater modeling has been a subject of research since Freeze and Harlan (1969) detailed and presented the physical processes and mathematical expressions occurring within a simplified version of the hydrologic cycle. The completed numerical simulations for the Bass Lake watershed offer attempts at examining the hydrologic cycle for a specific region and were completed using the HydroGeoSphere modeling code. The conclusions drawn from the simulation results are presented in the following section.

7.1 Final Conclusions

The simulation results for the Bass Lake model domain were compared to expected trends and observed field data. The groundwater heads and flow vector fields show general groundwater movement in expected directions and with reasonable flow velocities. The subsurface saturation levels behave as expected, showing the evapotranspiration component is withdrawing groundwater during plant transpiration.

The surface water depths and locations of water accumulation are consistent with known and collected field data. The surface water flow was shown to travel in appropriate directions at reasonable flow speeds. The simulated Bass Lake surface elevations were compared to observed surface water elevations. High overland friction values (for saturated and unsaturated simulations) overestimated the Bass Lake water level for the entire simulation period. Low overland friction values (for saturated and unsaturated simulations) produced Bass Lake water levels consistently within several centimeters of the observed values. However, all of the models overestimated the reaction of the water levels following major storm events. This overestimation could be due to the dynamic nature of natural processes (construction and destruction of beaver dams) occurring within the Bass Lake watershed. The presence of beaver dams likely has a profound impact on the Bass Lake water levels; however, their inclusion within a simulation model is a challenge for future research. The exchange fluxes between surface water and groundwater were found to occur at reasonable rates and at locations consistent with expectations.

The integrated surface water-groundwater model HydroGeoSphere ultimately produced acceptable simulations of the Bass Lake model domain. The construction and execution of the model was not without its issues. Following numerous modifications to the source code, to the model grid, and to the input parameters, HydroGeoSphere remains computationally burdensome. Future work should be conducted using large-scale real-world problems to continue testing the model applicability. Further source code and general model refinement are required to produce a robust and efficient integrated surface water-groundwater modeling program.

References

Atomic Energy of Canada Limited (AECL). (1994). *Environmental Impact Statement on the Concept for Disposal of Canada's Nuclear Fuel Waste*, AECL. Report No. AECL-10711, COG-93-1.

Beven, Keith J., (1996a). *A Discussion of Distributed Hydrological Modelling*, J. Distributed Hydrological Modelling, pp. 255-278.

Beven, Keith J., (1996b). *Response to Comment on: A Discussion of Distributed Hydrological Modelling,* J. Distributed Hydrological Modelling, pp. 289-295.

Bras, R.L. (1990). *Hydrology: An Introduction to Hydrologic Science*, Addison-Wesley, Massachusetts.

Brutsaert, W. (1984). *Evaporation in the Atmosphere: Theory, History and Applications*, D. Reidel, Dordrecht, The Netherlands.

Canadell, J., R.B. Jackson, J.R. Ehleringer, H.A. Mooney, O.E. Sala, and E.D. Schulze. (1996). *Maximum Rooting Depth of Vegetation Types at the Global Scale*, Oecologia p.583-595.

Cooley, R.L. (1971). *A Finite Difference Method for Unsteady Flow in Variably Saturated Porous Media: Application to a Single Pumping Well*, J. Water Resources, p.1607-1625.

Craig, R.F. (1997). *Soil Mechanics, 6th Edition*, E &FN Spon, Padstow, Cornwall, Great Britain.

District Municipality of Muskoka. (DMM). (2001). *State of the Lakes Report*, Bracebridge, Ontario.

Freeze, R.A and J.A. Cherry. (1979). *Groundwater*, Prentice Hall, New Jersey.

Graham, N.G. and M.B. Butts. (2005). *Flexible Integrated Watershed Modelling With MIKE SHE*, J. Watershed Models (to be published).

Havnø, K., Madsen, M.N. and J. Dørge. (1995) *MIKE 11 – A Generalized River Modelling Package*, J. Computer Models in Watershed Hydrology, p.809-846.

HydroGeoLogic, Inc. (2005). *MODHMS Software (Version 2.1) Documentation*, HydroGeoLogic, Inc., Herndon, Virginia.

Jyrkama, M.I. (2003). *A Methodology for Estimating Recharge*. PhD Thesis, Department of Civil Engineering, University of Waterloo, Waterloo, Ontario, Canada.

McDonald, M.G. and A.W. Harbaugh. (1988). *A Modular Three-Dimensional Finite-Difference Groudwater Flow Model*. US Geological Survey Techniques of Water-Resources Investigations, Book 6, Chap. A1, p.586.

McLaren, R. (2005a). *Grid Builder v.5.5*, Water Center for Groundwater Research, University of Waterloo, Waterloo, Ontario.

McLaren, R. (2005b). *Personal Communication re: HydroGeoSphere Development*, May 5th, 2005.

McKeon, B.J., J. Li, W. Jiang, J.F. Morrison, and A.J. Smits. (2004) *Further Observations on the Mean Velocity Distribution in Fully-Developed Pipe Flow*, J. Fluid Mech., 501, 135-147.

Ministry of Natural Resources Canada (MNR). (2002). *County of Muskoka Water Well Records*, Ministry of Natural Resources, Etobicoke, Ontario.

Ministry of Natural Resources Canada (MNR). (2005). *Ontario Land Cover Map (1:250,000)*, http://geogratis.cgdi.gc.ca/, accessed September 12th, 2004.

Ministry of Transportation Ontario (MTO). (2005*). Map 5: Huntsville, Bracebridge, Orillia, Peterborough, Barrie*, http://www.mto.gov.on.ca/english/traveller/map/, accessed June 1st, 2005.

Muskoka Lakes Association (MLA). (2004). *2004 Water Quality Testing Results – Raw Data*, Port Carling, Ontario.

National Aeronautics and Space Administration (NASA). (2004). *NASA Visible Earth*, http://visibleearth.nasa.gov/, accessed June 20th, 2004

Neuman, S.P. (1973). *Saturated-Unsaturated Seepage by Finite Elements*, ASCE J. Hydraulics, p. 2233-2251.

Oxtobee, J.P.A., and Novakowski, K. (2002). *A Field Investigation of Groundwater/Surface Water Interaction in a Fractured Bedrock Environment*. J. of Hydrology p. 169-193.

Panday, S. and P.Huyakorn. (2004). *A Fully Coupled Physically-Based Spatially-Distributed Model for Evaluating Surface/Subsurface Flow*, J. Advances in Water Resources 27 p. 361-382.

Pearsall, J. (2005). *Oxford Dictionary of English*, Oxford University Press.

Penman, H.L. (1948). *Natural evaporation from open water, bare soil and grass.*, Proc. R. Soc. London Ser. A, 193: 120-145.

Randall, J., Z. Ferreira, and R.R. Shepherd. (2003). *Development of Criteria and Design Constraints to Minimize Environmental Impacts of Golf Courses in Muskoka*, B.A.Sc. Honours Thesis, University of Waterloo, Waterloo, Ontario.

Refsgaard, J. C., Storm, B., and Abbott, M.B., (1996). *Comment on: A Discussion of Distributed Hydrological Modelling*, J. Distributed Hydrological Modelling, pp. 279-287.

Robin, M.J.L. and R.T. Schmidt. (1992). *FGEN Version 9.21 Cross-correlated Random Field Generator Truncated Fields in 3 or Fewer Dimensions*, Waterloo Centre for Groundwater Research.

Schroeder, P.R., T.S. Dozier, P.A. Zappi, B.M. McEnroe, J.W. Sjostrom and R.L. Payton. (1997). *The Hydrologic Evaluation of Landfill Performance (HELP) Model, Engineering Documentation for Version 3*, U.S. Army Corps of Engineers, Vicksburg, MS.

Scurlock, J.M.O., G.P. Asner, and S.T. Gower. (2001). *Worldwide Historical Estimates of Leaf Area Index*, 1932-2000, U.S. Department of Energy, Oak Ridge, Tennessee.

Shewchuck, Jonathan R. (2004). *Triangle: A Two-Dimensional Quality Mesh Generator and Delaunay Triangulator*, University of California at Berkeley, Berkeley California.

Sykes, J.F., S.D. Normani, and E.A. Sudicky. (2003). *Regional Scale Groundwater Flow in a Canadian Shield Setting, Ontario Power Generation*, Nuclear Waste Management Division, Report No. 06819-REP-01200-10114-R00.

Therrien, R., R.G. McLaren, E.A.Sudicky, and S.M. Panday. (2005). *HydroGeoSphere: A Three-dimensional Numerical Model Describing Fully-integrated Subsurface and Surface Flow and Solute Transport*, Groundwater Simulations Group, Waterloo, Ontario.

Turner, M. (2004). The *Determination of Flow Circulation Patterns in Bass Lake*, B.A.Sc. Honours Thesis, University of Waterloo, Waterloo, Ontario.

VanderKwaak, J. (1999). *Numerical Simulation of Flow and Chemical Transport in Integrated Surface-Subsurface Hydrologic Systems*, Ph.D. Thesis, University of Waterloo, Waterloo, Ontario.

Vardavas, I.M. (1987). *Modelling the Seasonal Variation of Net All-Wave Radiation Flux and Evaporation in a Tropical Wet-Dry Region*, J. Ecol. Model., 39: 247-268.